Deterministic Chaos and the Foundations of the Kinetic Theory of Gases

J. R. Dorfman

Institute for Physical Science and Technology and Department of Physics,

University of Maryland,

College Park, Maryland, 20742, USA

(February 5, 2008)

Recent work in dynamical systems theory has shown that many properties that are associated with irreversible processes in fluids can be understood in terms of the dynamical properties of reversible, Hamiltonian systems. That is, stochastic-like behavior is possible for these systems. Here we review the basic theory for this stochastic-like behavior and show how it may be used to obtain an understanding of irreversible processes in gases and fluids. Recent, closely related, work on the use of kinetic theory to calculate dynamical quantities such as Lyapunov exponents is also discussed.

I. INTRODUCTION

Dynamical systems theory [1], of which chaos theory is a part, has its origins in two famous problems of classical physics: to find a solution for the three body problem of celestial mechanics [2], and to find a proof of Boltzmann's ergodic hypothesis for the equivalence of time and ensemble averages of dynamical quantities (such as the force per unit area on the wall of the container) for isolated systems composed of a large number of particles [3]. In each case a great deal of progress toward an understanding of both the possibilities and difficulties in finding solutions to these problems has been made possible, over the past several decades, by the development of powerful and sophisticated mathematical and computer methods. These developments are well summarized in a number of excellent books and papers on dynamical systems theory, some of which are listed as Refs. [1,4–7] as well as references

contained therein. This article is a summary of a more extensive set of notes on this subject developed by the author which presents these topics in a somewhat more leisurely way, and also contains an extensive discussion of the Boltzmann transport equation [8]. Another discussion of many of these topics can be found in Ref. [9].

The purpose of this article is to explain some of these developments and to explore their application to the issues that preoccupied Boltzmann, namely the foundations of non-equilibrium statistical mechanics, with a particular emphasis on the foundations of the kinetic theory of dilute gases of particles that interact with short range forces [10–12]. The dynamical properties of such a dilute gas are somewhat easier to understand than those for other states of matter since in the main, the dynamics of a particle in a dilute gas consists of long periods of motion free from interactions with the other particles, punctuated by occasional and essentially brief collisions with other particles in the gas. That is, for a gas of particles with short range forces, the mean free time between collisions is much longer than the average duration of a collision. Even for such an apparently simple system complicated and difficult questions arise such as: How does one reconcile the reversible equations of motion with the irreversible macroscopic properties of such a system, particularly as seen in the Second Law of Thermodynamics concerning the irreversible increase of entropy? Why is the Boltzmann equation, which is admittedly derived on the basis of stochastic rather than mechanical assumptions, so successful in predicting the properties of dilute gases, and in explaining the origin of the hydrodynamic properties of the gas? and so on. This article will try to show how such questions might be answered by chaos theory and to indicate the general lines of the answers, to the extent that the issues are understood at present. Our discussions will be based at first upon the work of R. Bowen [13], D. Ruelle [4,14], and Ya. Sinai [15], who are the principal architects of the modern theory of the dynamical foundations of statistical mechanics. Recent developments due to major contributions of many other authors will also be described here, with appropriate, though certainly incomplete, references to the literature [16].

The plan of this article is as follows: In Section 2 we will review the basic ideas of

ergodicity and mixing for dynamical systems, and show their importance for statistical mechanics. We discuss the role of systems with few degrees of freedom, such as the baker's map and the Arnold cat map, as systems that exhibit ergodic and mixing properties and serve as paradigms for the kinds of properties we would like to see in systems with many degrees of freedom. The examples provided by such simple systems will motivate the important definitions of Lyapunov exponents, Kolmogorov-Sinai (KS) entropies, and hyperbolic, Anosov systems which will be important for the further discussions. In Section 3 we consider some recent applications of ideas from dynamical systems theory to the theory of transport phenomena, and illustrate the role of fractal structures that are responsible for diffusion and other transport processes. We consider there the application of escape-rate methods to transport theory, as developed by P. Gaspard and G. Nicolis [17], and the method of thermostatted dynamical systems, developed by D. Evans, W. Hoover, H. A. Posch, G. Morriss, and E. G. D. Cohen [18], as well as other authors. In Section 4 we use these ideas to present our current understanding of the dynamical origins of the Boltzmann equation, and to show how this equation, in turn, can be used to calculate quantities such as Lyapunov exponents which measure the chaotic nature of the relevant dynamics. We conclude in Section 5 with a number of remarks and questions.

This article is dedicated to the memories of T. H. Berlin, M. S. Green, M. Kac, J. Kestin, E. A. Mason, P. Resibois, and G. E. Uhlenbeck.

II. DYNAMICAL SYSTEMS THEORY AND STATISTICAL MECHANICS

We begin by recalling that classical statistical mechanics represents the mechanical state of a system of N point particles in $d-$dimensional space by a single point in a phase space of $2Nd$ dimensions, Γ-space, whose axes represent the position and momentum in each spatial direction for each of the N particles [19]. If we denote a point in Γ-space by $\mathbf{X}$, then the Newtonian motion of this phase point over a time t from $\mathbf{X}$ to $\mathbf{X}_t$ will be described by a time displacement transformation S_t with

$$\mathbf{X}_t = S_t(\mathbf{X}). \tag{1}$$

Although statistical mechanics is usually concerned with systems where N is large and t is continuous, usually called "flows", here we will often consider simple dynamical systems in phase spaces of two dimensions and where the time t takes on discrete values. Such low dimensional systems with discrete time steps are called "maps" [1,7]. The reason for considering them is that they display the kind of dynamical properties that we would like to find in systems of more interest to physicists. In particular we would like to identify the important features of these simple maps which are responsible for such properties as ergodic behavior and an approach to an equilibrium state, and then see if such properties are characteristic of more general flows for more realistic models of physical systems.

A. Invariant Measures

Having defined the phase space Γ and the time displacement operator for either continuous or discrete times, we now add a third basic quantity to our discussion, an invariant measure, $\mu(A)$, where A is some set in phase space. A measure μ is invariant under the time displacement operator S_t if for any set A, $\mu(A) = \mu(S_{-t}A)$, i.e. the measure of the pre-image of A, denoted by $S_{-t}A$ is equal to the measure of A for any $t > 0$. This condition, that an invariant measure be constant under time evolution, is closely related to the usual statements in equilibrium statistical mechanics where we append to the evolution equation for the Liouville distribution function, $\rho(\mathbf{X}, t) = \rho(S_{-t}(\mathbf{X}, 0)$, the requirement that ρ be independent of time. An example of the point of the requirement that $t > 0$, will be seen shortly when we consider invariant measures for one dimensional maps, which are not invertible. Well known examples of invariant measures include the volume of a set in Γ-space which defines the Liouville measure, $\mu_L(A)$,

$$\mu_L(A) = \int_A d\Gamma, \tag{2}$$

where the integration is over the range of position and momentum coordinates that define the set A in Γ-space; the microcanonical measure on the constant energy surface, $\mu_{m.c.}(A)$, defined by

$$\mu_{m.c.}(A) = \int_A \frac{d\Omega}{|\nabla H|}, \tag{3}$$

where $d\Omega$ is a surface element on the microcanonical energy surface, and ∇H is the gradient of the Hamiltonian H of the system with respect to all of the coordinates and momenta in Γ-space [19].

There are a number of useful systems of low dimensionality with simple invariant measures, as well. As they will be used in our further discussions, we describe the systems and their appropriate invariant measures now. We should mention that very often dynamical systems have infinitely many invariant measures. However of these, usually only one, called the natural or SRB measure, can be used to compute the type of ensemble averages used in statistical mechanics. The other measures are often defined on very special points or sets in phase space. For example, one can define invariant delta function measures on periodic points of the system, but these measures can not generally be used to characterize the statistical properties of the system. In all of the disussions to follow we will assume that the total measure of the appropriate phase space is finite, which implies, of course, that the measure of any subset of the space is finite.

The simplest map with an invariant measure is a piecewise linear, 1-d non-invertible map of the unit interval, $[0, 1]$ *onto* itself, an example of which is the tent map illustrated in Fig. 1. This map is given by [1,7]

$$\begin{aligned} x_{n+1} &= 2x_n \quad \text{for} \quad 0 \le x_n < 1/2, \\ &= 2(1 - x_n) \quad \text{for} \quad 1/2 \le x_n \le 1 \end{aligned} \tag{4}$$

Here the invariant measure of a set such as A, $\mu(A)$ illustrated in the figure is its Lebesgue measure, or simple area, $\mu_l(A)$. For this map the pre-image of A is the union of two sets each of Lebesgue measure $\mu_l(A)/2$. Note that the image of A typically has Lebesgue measure $2\mu_l(A)$, so our definition of the invariant measure, using the condition $t > 0$ above allows

us to define such measures even for non-invertible maps, such as the tent map. an invariant measure should be defined by considering the pre-image of A, as we did above.

For our purposes the most useful maps will be two dimensional $(2-d)$ invertible maps, particularly, the baker's map illustrated in Fig. 2, and the toral automorphism, often called the Arnold cat map, illustrated in Fig. 3. [20]. The baker's map is defined on the unit square $0 \leq x, y \leq 1$ by the dynamical equation

$$\begin{aligned}\begin{pmatrix} x_{n+1} \\ y_{n+1} \end{pmatrix} &= \mathbf{B} \begin{pmatrix} x_n \\ y_n \end{pmatrix} \\ &= \begin{pmatrix} 2x_n \\ y_n/2 \end{pmatrix} \text{ for } 0 \leq x < 1/2, \text{and} \\ &= \begin{pmatrix} 2x_n - 1 \\ (y_n+1)/2 \end{pmatrix} \text{ for } 1/2 \leq x \leq 1. \end{aligned} \tag{5}$$

This map has an invariant measure which is just the Lebesgue measure of two-dimensional regions on the unit square. This follows immediately from the observation that horizontal lengths become twice as long, but vertical lengths become one half as long. One can also define the inverse map $\mathbf{B}^1$ in a simple way. Under the inverse map, horizontal lengths contract by a factor of 2, and vertical lengths become twice as long.

Toral automorphisms, $\mathbf{T}$, are defined in general by the transformation

$$\begin{pmatrix} x_{n+1} \\ y_{n+1} \end{pmatrix} = \mathbf{T} \cdot \begin{pmatrix} x_n \\ y_n \end{pmatrix} = \begin{pmatrix} a & b \\ c & d \end{pmatrix} \cdot \begin{pmatrix} x_n \\ y_n \end{pmatrix} \mod 1, \tag{6}$$

where a, b, c, d are positive integers, and the determinant of the 2×2 matrix, $ac - bd = 1$. Thus a unit torus is mapped onto a unit torus, and the condition on the determinant guarantees that all areas on the unit torus are preserved by the mapping. For reasons to be clear shortly, we will restrict our attention here to so-called hyperbolic maps where the eigenvalues of $\mathbf{T}$ do not lie on the unit circle. The Arnold cat map is a particular case of this where the matrix $\mathbf{T}$ is given as $\begin{pmatrix} 2 & 1 \\ 1 & 1 \end{pmatrix}$. This is the case illustrated in Fig. 3.

B. Ergodic and Mixing Systems

For classical systems, the foundations of equilibrium statistical mechanics are based upon Boltzmann's *ergodic hypothesis*: The long time average of the dynamical quantities accessible to measurement, such as the force per unit area exerted by a fluid on the walls of a container, for an individual, isolated system, is equal to the ensemble average of the same dynamical quantity taken with respect to a microcanonical ensemble [19]. One of the tasks of dynamical systems theory is to identify the kinds of dynamical systems and dynamical quantities for which the ergodic hypothesis can be verified.

The first major result in this direction was Birkhoff's ergodic theorem [20,21]: Consider some dynamical function, $F(\mathbf{X})$, defined on the constant energy surface, $\mathcal{E}$, that satisfies the condition

$$\int d\mu F(\mathbf{X}) < \infty, \tag{7}$$

where the integration is with respect to the microcanonical measure defined in Eq. (3), and is carried out over the whole surface. Suppose further that the total measure of the surface is finite. Then: (i) the time average of F, denoted by $\bar{F}(\mathbf{X}) = \lim_{T\to\infty} \frac{1}{T} \int_0^T dt F(\mathbf{X}(t))$ exists almost everywhere on the constant energy surface, that is, for almost every starting point $\mathbf{X}$; (ii) The time average $\bar{F}(\mathbf{X})$ may depend on the particular trajectory but not upon the initial point of the trajectory; (iii) The ensemble average of $\tilde{F}$ is equal to ensemble average of F itself. That is, $\int d\mu F(\mathbf{X}) = \int d\mu \bar{F}(\mathbf{X})$; and (iv) One can replace the entire constant energy surface as the region of integration by any invariant subset of non-zero measure. Here an invariant set is one where all points (with the exception of a subset of measure zero) initially in the set remain in the set during the course of their time evolution, and the measure of the set does not change with time. Birkhoff's theorem does not show that systems of physical interest are ergodic in the sense of Boltzmann because the time average of an integrable dynamical quantity may depend on trajectories and thus not necessarily be equal to an ensemble average, which is, of course, just a number. We therefore define

an ergodic system to be one where the time average $\bar{F}$ of any dynamical quantity F is a constant on the surface. For such a system the time average of F is indeed its ensemble average, which we denote by $\tilde{F}$, since

$$\int d\mu F(\mathbf{X}) = \bar{F} \int d\mu, \tag{8}$$

from which it follows that

$$\bar{F} = \frac{\int d\mu F(\mathbf{X})}{\int d\mu} = \tilde{F}. \tag{9}$$

It should be remarked that although it is true that for ergodic systems the ensemble average of any integrable function is equal to its time average, the requirement of ergodicity may be demanding too much of the dynamical systems to which we would like to apply equilibrium statistical mechanics. For example, for applications of statistical mechanics we might restrict ourselves to a smaller class of functions for which we would need to prove the equivalence of time and ensemble averages, thus placing fewer demands on the dynamics.

Over the seventy or so years since Birkhoff's theorem was proved, a number of systems have been shown to be ergodic [15,16,22]. These include simple transformations of the unit interval $[0, 1]$ onto itself by $x' = x + \alpha \mod 1$, (think of taking steps of length α on a circle of unit circumference) where α is irrational, the baker's map, toral automorphisms of the type described above, geodesics on surfaces of constant negative curvature, and of most interest for physics, billiard ball systems in two and three dimensions. These systems include a particle moving among a system of fixed, non-overlapping hard disk or hard sphere scatterers (the Lorentz gas) [15], as well as certain systems of moving hard disks or hard spheres, in a box with periodic boundary conditions [23]. The proofs of ergodicity for billiard systems are not at all easy(!), but billiards may be the simplest physically realistic systems to analyze because of the simplicity of the collisions of the particles [24]. We will return to this point further on, but first we wish to develop further characterizations of the dynamical systems for which the methods of statistical mechanics apply.

Gibbs took Boltzmann's ideas a step further by introducing the idea of a *mixing* system [16,19,20]. He proposed to look at an initial ensemble of mechanically identical systems all

with the same total energy, but with different initial conditions. Suppose the phase points for this ensemble are confined, initially to a set of positive measure, A, on the constant energy surface, $\mathcal{E}$. Then in the course of time this set will evolve to a new set, A_t, with the same measure as A. A system is called mixing in the sense of Gibbs, if for any fixed set B of positive measure on $\mathcal{E}$

$$\lim_{t\to\infty} \frac{\mu(B \cap A_t)}{\mu(B)} = \frac{\mu(A)}{\mu(\mathcal{E})}. \tag{10}$$

That is, a system is mixing if the time evolution of any set of non zero measure leads to the set being distributed uniformly with respect to the invariant measure μ over the constant energy surface.

It is easy to show that the condition that a dynamical system be mixing is stronger than requiring that it be ergodic [16,20]. That is, all mixing systems are ergodic but not *vice versa*. For example the ergodic transformation of the unit interval $[0, 1]$ onto itself, by $x' = x + \alpha \mod 1$, for irrational α is not mixing. To see this just let A, B each be small connected sets of the unit interval, and consider the set $C_n = A_n \cap B$, the intersection of B with the image of A after n applications of the transformation. The limit of $\mu(C_n)$ as n gets large is not well defined and the set A does not get uniformly mixed over the unit interval, but instead moves as a rigid set without mixing.

The mixing property of a dynamical system is even more interesting for our purposes than that of ergodicity, not only because mixing implies ergodicity, but also because if a system is mixing, then non-equilibrium ensemble averages approach their equilibrium values as time gets large [8,20]. That is, if one starts with some non-equilibrium ensemble distribution on $\mathcal{E}$, not the microcanonical one, and if this distribution is a measureable function on $\mathcal{E}$, then the time evolution of this distribution function is governed by Liouville's equation. The ensemble average of any measurable dynamical quantity, F, at some time t is then determined by the integral of F with respect to the distribution function at time t. For a mixing system, this ensemble average approaches its value in the microcanonical ensemble as t approaches infinity. Physically this means that in a weak sense, that is, under integration with some

well behaved function , non-equilibrium distribution functions approach the microcanonical equilibrium distribution in the long time limit. This is the essential information needed for the validity of non-equilibrium statistical mechanics.

Systems that have been rigorously proved to be mixing include the baker's map, the hyperbolic toral automorphisms, and the Lorentz gases described above [16,25,26]. There is little doubt the moving hard sphere, or hard disk systems are mixing, but as yet there is no rigorous proof of this supposition.

C. Dynamics, Symbolic Dynamics, and Lyapunov Exponents

While we will not prove here that the baker's map or the toral automorphisms are mixing systems, it is very instructive to sketch the lines of the proof for the baker's map. This will provide a simple example of a *Markov partition*, which is a useful construction in many other, and more general, contexts [27,28]. We begin by noting that any number in the interval $[0,1]$ can be expressed in a binary series, the dyadic expansion, as

$$x = \frac{a_0}{2} + \frac{a_1}{2^2} + \frac{a_2}{2^3} + \cdots, \tag{11}$$

where each of the a_i can take on the values $0, 1$, depending on x, of course. We can represent x as an infinite sequence of 0'and 1's as

$$x = (a_0, a_1, a_2, \cdots). \tag{12}$$

This representation is unique except for those fractions whose representations consist of a finite number of a's followed by an infinite number of 0's or of 1's. Such fractions have two equivalent representations, one with an infinite sequence of zeroes and one with an infinite sequence of 1's. As these particular fractions form a countable set, we can always require that we use one of these representations for them consistently. In a similar manner we may represent y in $[0,1]$ as

$$y = \frac{b_{-1}}{2} + \frac{b_{-2}}{2^2} + \cdots \text{ or}$$
$$y = (b_{-1}, b_{-2}, \cdots). \tag{13}$$

Combining these two representations, we see that any number in the unit square $0 \leq x, y \leq 1$ may be expressed by

$$(x, y) = (\cdots b_{-2} b_{-1} . a_0 a_1 a_2 \cdots), \tag{14}$$

where we have separated the x-sequence from the y-sequence by a "dot", and strung the y-sequence to the left, with the x-sequence to the right. We can clearly approximate any point in the unit square to an accuracy 2^{-N} by a finite sequence

$$(x, y) \simeq (b_{-N} b_{-N+1} \cdots b_{-1} . a_0 a_{-1} \cdots a_{N-1}). \tag{15}$$

Such an approximation is equivalent to locating the point somewhere in one of the small squares obtained by dividing the unit square into small regions by drawing vertical lines at intervals of 2^{-N}, and similarly with horizontal lines. This partition of the unit square into much smaller regions, is an example of a Markov partition, because of the particular way in which the lines are drawn, as we explain below. The approximation to the point (x, y) consists in specifying the particular small region in which the point is located. This procedure for approximating a particular point in phase space, here the unit square, is a mathematical echo of the idea of coarse graining often used in statistical mechanics.

The central feature that we now want to emphasize is that given the representation of the point (x, y) on the unit square by Eq. (14), its image, (x', y') under the baker's map becomes

$$(x', y') = (\cdots b_{-2} b_{-1} a_0 . a_1 a_2 \cdots), \tag{16}$$

where all the members of the sequence have shifted one unit to the left, and, in particular, the number a_0 has moved past the "dot" into the y-sequence. Thus we have mapped a deterministic dynamical system onto something that looks like a "coin toss" experiment. A point on the unit square can be mapped onto a bi-infinite sequence of 0's and 1's, that is, onto a particular realization of a bi-infinite coin toss sequence, and the "dot" indicates the location of one particular moment in the sequence of tosses. The next toss will simply

be the next step in the process of generating the entire sequence, and corresponds, in the baker's map, to one iteration of the map! A coin toss experiment is, of course, a stochastic process, with a given probability p for obtaining a "heads" and $q = 1 - p$ for a "tails". Our ability to map certain deterministic dynamical systems onto random, stochastic processes is the main point of this article! Of course the central question is to identify those systems for which such a mapping is possible.

Now consider what happens to all of the points in the small square of order 2^{-N} on a side, which we will take to be the set A in the Gibbs picture. We know that for all such points the values of $b_{-N}, b_{-N+1}, \cdots, b_{-1}, a_0, a_1, \cdots, a_{N-1}$ will be the same. However, each of the additional, unspecified $a_{N+k}, b_{-N-k'}$, with $k > -1, k' > 0$, can take on the values 0 or 1. All of the points in the small square correspond to all possible values of these unspecified a's and b's. After N iterations of the baker's map, all of the specified values for the a's will have shifted onto the y coordinate, and the set of points in the original small square will be uniformly distributed along the x interval $[0, 1]$. After $2N$ iterates of the map, we will have lost track of the y coordinates as well, at least to the accuracy we have specified, and the points originally confined to our small square will be uniformly distributed over the entire unit square. Thus the system is indeed mixing. Note also that a similar circumstance would apply if the map were run backward, and the sequence shifted to the right past the "dot" at each step. Thus we can see an approach to a uniform distribution for both the "forward" and the "time reversed" motions. Consequently we can say that it is certainly possible for the ensemble distribution for a reversible dynamical system to show an approach to a uniform, equilibrium state for both forward and backward motions, provided we look at the distribution on a slightly coarse grained scale.

A very similar analysis applies to the hyperbolic toral autormophisms, but the partitioning of the unit square (or torus) should be done with lines whose directions and spacings are dictated by certain features of the particular automorphism [16,27]. These features will be determined by the directions of the stable and unstable manifolds, and by the Lyapunov exponents of the map, all of which we will discuss shortly. The representation of the trajec-

tory of a point on the unit square under the baker's map in terms of sequences of 0's and 1's, is an example of *symbolic dynamics*, whereby, trajectories are coded into sequences whose elements are chosen from a finite number of symbols (here 0 or 1) [1,7,16]. The representation of dynamics using such sequences can be very useful in analyzing and calculating the properties of dynamical processes in simple enough systems. For example, readers might convince themselves that the Cantor "middle third" set can be coded by similar sequences of two symbols. (Hint: Consider the map $x' = 3x \mod 1$, and represent all numbers on the unit interval by a series in inverse powers of 3, with coefficients $0, 1, 2$. The "middle third" Cantor set is isomorphic to all sequences where a 1 never appears, and the above transformation just maps this set onto itself.)

Now a remarkable thing has just happened in our analysis of the baker map. We started with a set of points that were all within a distance $\epsilon = 2^{-N}$ of each other, and they spread out over the unit square. Consequently, the rates and directions of separation, or conversely of approach, of the images of two nearby points are certainly quantities of some interest for understanding the mixing process. For the baker's map, it is clear that the images of infinitesimally close points with the same y coordinate will separate in the x-direction, so that their separation, d_n, after n steps will be $2^n d_0$, where their initial infinitesimal separation is d_0. However, the images of two infinitesimally close points with the same x coordinate will approach each other as $d_n = 2^{-n} d_0$. The images of two infinitesimally close points that do not lie in a strictly vertical line will also separate exponentially, since the exponential separation in the x - direction will dominate the separation of the two points. Consequently, the images of any two infinitesimally close points will separate exponentially, except for a set of measure zero, namely those points with the same y coordinate. If we consider the time reversed motion, then points will separate in the y direction, approach in the x-direction, but the images of almost all nearby points will separate exponentially rapidly. The exponents that govern the rates of exponential separation or approach are called *Lyapunov exponents* [1,4]. We see that the baker's map has two Lyapunov exponents, $\ln 2, -\ln 2$. The fact that the sum of these exponents is zero is not accidental, it is a consequence of the

invariance of the Lebesgue measure on the unit square. Moreover, while the separation of the nearby points is exponential for a large number of iterations of the map and the rate of separation is given by the Lyapunov exponents on this time scale. However this exponential rate of separation cannot continue forever since the measure of the phase space is finite.. Eventually the separation will become large enough that the folding mechanisms of the baker map will take over and the two points will find themselves in very different regions of the unit square. In general we will find that exponential separation of trajectories in a bounded phase space cannot continue indefinitely, but that there is always a folding mechanism that keeps trajectories within the bounded region.

Consider now the case of the hyperbolic toral automorphisms, Eq. (6), and let us use the Arnold cat map as an example. An elementary calculation shows that the 2×2 matrix given below Eq. (6) has the eigenvalues $\Lambda_\pm$ given by

$$\Lambda_\pm = \frac{3 \pm 5^{1/2}}{2}. \tag{17}$$

Notice that $\Lambda_+ > 1, \Lambda_- < 1$, and the invariance of the Lebesgue measure on the unit torus requires that $\Lambda_+\Lambda_- = 1$. Here again we see that there is an expanding direction which is determined by the direction of the eigenvector corresponding to Λ_+, and a contracting direction determined by the direction of the eigenvector corresponding to Λ_-. The associated Lyapunov exponents which we denote by $\lambda_\pm$ are given by $\lambda_\pm = \ln \Lambda_\pm$. Here again we note that the invariance of the measure on the unit torus requires that $\lambda_+ + \lambda_- = 0$. Consider a typical point on the unit square and draw a set of lines through it such that one is in the direction of the expanding eigenvector and the other is in the direction of the contracting eigenvector. We will refer to these two lines as the *expanding or unstable manifold* and the *contracting or stable manifold* respectively. The images of two infinitesimally close points on the unstable manifold will separate exponentially, while the images of two close points on the stable manifold will approach exponentially [1,16].

Now we can return to the idea of a Markov partition mentioned at the beginning of this section. A Markov partition is a partition of the phase space into a finite collection

of small "parallelograms" with disjoint interiors and whose sides lie on stable and unstable manifolds, perhaps suitably extended, of points in the space. For the case of the baker's map, the parallelograms have vertical and horizontal sides, while for the Arnold cat map, the parallelograms have sides that lie along the eigen directions of the matrix below Eq. (6). The existence of a Markov partition for a dynamical system allows one to use symbolic dynamics to code the trajectories, and to use of the theory of Markov processes to analyze the time dependence of distribution functions defined on the phase space. For example, the solution of the Perron-Frobenius equation to be discussed in Section 4 is greatly facilitated if one can construct a suitable Markov partition for the system. The calculations described in Section 3.4 makes extensive use of the method of Markov partitions. Further details and a discussion of the use of Markov partitions to compute other quantities of dynamical interest such as Kolmogorov-Sinai entropies, to be discussed below, can be found in Refs. [15,16].

In order to show that the Lyapunov exponents are non-zero for both the baker map and the hyperbolic toral automorphisms we have had to calculate them, thus, given a dynamical system, it is not always obvious that it will have the positive Lyapunov exponents that are required for the exponential separation of trajectories.

We can generalize the concept of Lyapunov exponents, stable, and unstable manifolds to higher dimensional systems and to flows, in addition to maps [4]. Usually the only fundamental difference between maps and flows is that flows typically have one zero Lyapunov exponent in the direction of the trajectory in phase space [5,4]. Although the proof can sometimes be involved mathematically, the zero Lyapunov exponent in the direction of the trajectory can be understood by imagining two infinitesimally close points that lie on the same trajectory in phase space. If the dynamics of the system consists of free particle motion punctuated by collisions that are instantaneous or almost so in comparison with other time scales of the system (the mean free time between collisions, say), then the two points will remain close over the course of their motion and their separation will certainly not be exponential. Furthermore, if the dynamics is consistent with an invariant measure, such as Hamiltonian dynamics, then the sum of *all* the non-zero Lyapunov exponents must be zero

as a consequence of the invariance of the measure. This suggests that the Lyapunov exponents should be defined in such a way as to be consistent with the invariance of the measure, which is the case in the two examples we have considered. It is worth pointing out that Lyapunov exponents for periodic trajectories, which have delta function invariant measures, may very well be different from those defined with respect an invariant measure defined on the entire phase space. One additional property of the non-zero Lyapunov exponents for a Hamiltonian system that is important is the *symplectic conjugate pairing rule*. That is, for a system with symplectic dynamics, the non-zero Lyapunov exponents, should there be any, must come in "plus-minus" pairs, with each pair of exponents summing separately to zero, independent of the values of the other pairs. This is a consequence of the symplectic form of Hamilton's equations of mechanics [29], and is not true for reversible systems that are not symplectic. We shall encounter such systems in the further sections.

D. The Kolmogorov-Sinai Entropy

Let us now look at some properties of the Arnold cat map in more detail. In Fig. 4, we show an initial set A which is located in the lower right hand corner of the unit square, and in Figs. 5, 6, 7, we show the evolution of this set after 2, 3, and 10 iterations of the map respectively (a similar set of figures can be found in [30]). As the number of iterations increases the set becomes longer and thinner such that at the third iteration the set has begun to fold back across the unit square, and after 10 iterations the set is so stretched and folded that it appears to cover the unit square uniformly. If we were able to increase the resolution of this illustration beyond the 10^5 points used to generate it, we would see that this apparently uniform distribution is made up of very many, on the order of 10^6, thin lines parallel to the expanding direction of the cat map, and very close together. Since the initial square is getting stretched along the unstable manifold, at every iteration we learn more about the initial location of points within the small initial set A. That is, suppose we can distinguish two points on the unit square only if they are separated by a distance δ, the

resolution parameter, and suppose further that the initial set has a characteristic dimension on the order of δ [9]. We cannot resolve two points in the initial set then, but after a time t, the initial set will have stretched along the unstable direction to a length on the order of $\delta \exp(\lambda_+ t)$, and we can easily resolve the images of points in the initial set. Thus as we look at the successive images of the initial set we are able to obtain more and more information about the location of points in the initial region, in fact, the information is growing at an exponential rate. The exponential rate at which information is obtained is measured by the *Kolmogorov-Sinai (KS) entropy* [1,4,16] , h_{KS}, and for our simple system, the cat map, $h_{KS} = \lambda_+$. In general, one finds that for a dynamical system of several dimensions, with positive Lyapunov exponents, and where all of the points are confined to a bounded region of phase space, then

$$h_{KS} = \sum_i \lambda_{+,i}, \tag{18}$$

where the summation is over all of the positive Lyapunov exponents of the system. Eq. (18) is referred to as Pesin's theorem [4,31], and we mention that there is a highly developed theory for the KS entropy [16,27], which we cannot expand upon here. We mention again that the Lyapunov exponents and the KS entropy should be defined with respect to an invariant measure. Thus, there may be many sets of exponents for a single system, e.g., Lypaunov exponents defined on periodic orbits may differ from those defined with respect to the natural invariant, or SRB, measure, which will be discussed in Sec. 2.5. Pesin's theorem applies if h_{KS} and the Lyapunov exponents are defined with the respect to the natural invariant measure. In the next section we will consider a situation where points can escape from a bounded phase space region, and where the KS entropy is less than the sum of the positive Lyapunov exponents by an amount that is equal to the escape rate of points from the bounded region. One might say that in this latter case the rate of stretching is slightly greater than the rate of folding.

E. Hyperbolic and Anosov Systems

We have argued that both the baker's map and the hyperbolic toral automorphisms are mixing systems, and as a consequence, as simple models of dynamical systems, they show an approach to equilibrium. In fact we can map these simple reversible dynamical systems onto stochastic processes. The mechanisms responsible for this desirable behavior are: (1) the exponential separation of trajectories in phase space, characterized by positive (with corresponding negative) Lyapunov exponents with corresponding expanding and contracting directions; and (2) the folding of phase space regions during their time evolution due to the boundedness of the phase space, leading to a uniform distribution of points over the phase space, at least on a coarse grained scale. It is now time to formalize these properties so that we can see if the above mechanisms apply for more realistic systems.

To do this we consider a general dynamical system with several degrees of freedom, with an associated phase space Γ and an invariant measure μ on the phase space. Let us write the equations of motion for the phase space variables, denoted by $\mathbf{X}$ as

$$\dot{\mathbf{X}} = \mathbf{G}(\mathbf{X}), \tag{19}$$

where, typically, but not always, $\mathbf{G}$ is the appropriate derivative of the Hamiltonian function with respect to the phase space variables. In order to consider the possible exponential separation of infinitesimally nearby trajectories, we consider the time evolution of a small displacement $\delta\mathbf{X}$ in phase space between two arbitrarily close points [5,32]. This displacement satisfies a linearized equation in the tangent space to Γ at the point $\mathbf{X}$,

$$\delta\dot{\mathbf{X}} = \frac{\partial \mathbf{G}(\mathbf{X})}{\partial \mathbf{X}} \cdot \delta\mathbf{X}. \tag{20}$$

The solution to this equation in the tangent space has the form

$$\delta\mathbf{X}_t = \mathbf{M}(t, \mathbf{X}) \cdot \mathbf{X}, \tag{21}$$

where $\mathbf{M}$ satisfies the equation

$$\dot{\mathbf{M}}(t,\mathbf{X}) = \frac{\partial \mathbf{G}(\mathbf{X}_t)}{\partial \mathbf{X}_t} \cdot \mathbf{M}(t,\mathbf{X}). \tag{22}$$

The matrix $\mathbf{M}$ plays a special role in the discussion now, as it determines the dynamical evolution of the displacements in the tangent space.

We define an *Anosov* dynamical system as a map or flow with the following properties [6,16,33] (we consider flows here, but our definition can be easily modified for maps):

1) for almost every point, $\mathbf{X}$, in the phase space Γ, there is a decomposition of the tangent space at $\mathbf{X}, \mathcal{T}\Gamma(\mathbf{X})$, into three subspaces, an unstable subspace $\mathcal{E}^u_X$, a stable subspace $\mathcal{E}^s_X$, and a center subspace $\mathcal{E}^n_X$ such that

$$\mathcal{T}\Gamma(X) = \mathcal{E}^u_X \oplus \mathcal{E}^s_X \oplus \mathcal{E}^0_X. \tag{23}$$

2)There are constants C_s, C_u, and Λ with $C_s, C_u > 0$, and $0 < \Lambda < 1$, such that:

a) If $\delta\mathbf{X}$ is in $\mathcal{E}^s_X$, then

$$||\mathbf{M}(t,\mathbf{X}) \cdot \delta\mathbf{X}|| \leq C_s \Lambda^t ||\delta\mathbf{X}||, \tag{24}$$

b) If $\delta\mathbf{X}$ is in $\mathcal{E}^u_X$, then (for $t > 0$)

$$||\mathbf{M}(-t,\mathbf{X}) \cdot \delta\mathbf{X}|| \leq C_u \Lambda^t ||\delta\mathbf{X}||, \tag{25}$$

c)The subspaces $\mathcal{E}^u_X, \mathcal{E}^u_X, \mathcal{E}^0_X$ vary continuously with $\mathbf{X}$. This means that any vector $\delta\mathbf{X}$ can be written as

$$\delta\mathbf{X} = \delta\mathbf{X}^u_X + \delta\mathbf{X}^s_X + \delta\mathbf{X}^0_X, \tag{26}$$

where each term is in the indicated subspace. Then each of the $\delta\mathbf{X}^j_X$ vary continuously with $\mathbf{X}$.

d)The various subspaces intersect transversely, without any tangencies.

The center subspace contains the directions of motion with zero Lyapunov exponent, such as the direction tangent to the trajectory of the system in phase space, and any other directions associated with the macroscopically fixed constants of motion, such as the total

momentum, etc. Note that in condition b) above we considered the time reversed motion on the unstable manifold, and the condition is that small deviations from the orbit converge exponentially to zero for the time reversed motion, while for the stable manifold, the deviations approach zero exponentially in the forward direction. The transversality condition d) assures that there are no tangencies among the subspaces which would greatly complicate the description of the dynamics.

As we will see in the next section, there are a number of circumstances of physical interest where we will need to consider invariant subregions of the full phase space. These regions are usually fractal attractors or repellers, to be defined and described in the next section, which have Lebesgue measure zero in the full phase space. It may happen that the dynamics, when restricted to such an invariant subregion still satisfies conditions a)-d) above. In such a case we say that the dynamics is *hyperbolic* on the subregion. An Anosov system, then, is one which is hyperbolic on the full phase space.

Anosov systems of finite total measure have the properties that we need for equilibrium and non-equilibrium statistical mechanics, they are ergodic and mixing, with positive KS entropy. However with the exception of the simple models we have discussed already, we do not know if some of the most physically realistic systems are Anosov. Certainly hard disk or hard sphere systems are not Anosov, since the collision dynamics produces discontinuities in which one member of a pencil of nearby trajectories just includes a grazing collision involving two particles, but many of the other trajectories miss that collision altogether. However, Sinai and co-workers have shown that such systems still have many of the nice properties of Anosov systems [15,24]. In view of the difficulty in establishing whether a physical system is Anosov, Gallavotti and Cohen [34] have proposed a *chaotic hypothesis*, namely, that until one proves that a system of interest is not Anosov, one should assume that it is, and then calculate its dynamical properties based upon that supposition. Their reasoning is simply that had we waited for someone to prove that a given physical system is ergodic before applying the methods of equilibrium statistical mechanics to it, there would have been precious little progress in understanding the properties of equilibrium systems over

the last hundred years. Thus it would seem practical for physicists, at least, to compute the dynamical properties of systems by assuming that the systems are Anosov. We will adopt this attitude here, for the most part, but we will also treat the hard disk Lorentz gas in the later sections, and make explicit use of the discontinuous dynamics. We'll see that the failure of this system to be Anosov is not a serious handicap.

We conclude this section with the statement of an important theorem due to Sinai, Ruelle, and Bowen, [6] that is a generalization of the ergodic theorem to general hyperbolic systems, whether they be an Anosov system, or a system which is restricted to a repeller or an attractor. Suppose then that we have: (1) a hyperbolic system described by a flow $\mathbf{X}_t = S_t(\mathbf{X})$ for almost all $\mathbf{X}$ in some invariant region $\mathcal{R}$, and (2) $g(\mathbf{X})$ is a continuous function of $\mathbf{X}$. Then there exists a unique measure μ such that for almost all (with respect to Lebesgue measure) $\mathbf{X}$ in $\mathcal{R}$

$$\lim_{T\to\infty} \frac{1}{T}\int_0^T dt g(S_t(\mathbf{X})) = \frac{\int g(\mathbf{Y})d\mu}{\int d\mu}, \tag{27}$$

where the integrals on the right hand side of Eq. (27) are over the invariant region $\mathcal{R}$. The measure that is proved to exist by this SRB theorem is called a SRB measure. In the case that $\mathcal{R}$ is the full phase space Γ, then the SRB measure is the microcanonical measure, and the SRB theorem is equivalent to the statement that Anosov systems are ergodic. However the theorem is much more general than that, and as we have said, it applies to hyperbolic attractors and repellers, as well.

III. APPLICATIONS OF DYNAMICAL SYSTEMS THEORY TO TRANSPORT: REPELLERS AND ATTRACTORS

A. The Escape-Rate Method

In our discussion of the KS entropy, we argued, in effect, that if we have a closed hyperbolic or Anosov system, the sum of the positive Lyapunov exponents is equal to the KS

entropy (Pesin's theorem, Eq. (18)). Suppose now that we have a situation frequently encountered in transport phenomena, where particles can escape from the system. Consider, for example, the diffusion of particles in a fluid, that has absorbing boundaries. In that case, particles that reach the boundary will be lost from the system. Here we argue that it is possible to apply dynamical systems theory to such a case, and that this application shows a deep connection between transport coefficients and the properties of chaotic dynamical systems. This connection was first made by Gaspard and Nicolis [17]. This is an appropriate place to say that by a chaotic dynamical system we mean one that has a positive KS entropy, i.e., exponential separation of trajectories, and a bounded phase space so that folding takes place.

First we consider the macroscopic description of such a diffusion phenomena. Suppose we have some macroscopic region of characteristic size L, much greater than any of the microscopic lengths that characterize the system. Suppose that the system consists of one moving particle and a collection of fixed scatterers, arranged in such a way that the moving particle is never trapped inside the system. Now suppose that the boundary of the system is absorbing, so that any particle that reaches the boundary will be absorbed, and removed from the system. The macroscopic description of this process is through the Fokker-Planck equation for $P(\vec{r},t)$, the probability of finding the particle at point $\vec{r}$ at time t, which is

$$\frac{\partial P(\vec{r},t)}{\partial t} = D\nabla^2 P(\vec{r},t), \tag{28}$$

supplemented by the absorbing boundary condition, $P = 0$ on the boundary. (In this case the Fokker-Planck equation coincides with thediffusion equation.) Here the quantity of interest is the diffusion coefficient D. If we solve this equation and ask for the probability that the particle will still be in the system at time t, $P(t) = \int d\vec{r} P(\vec{r},t)$ we find that $P(t) = \exp[-\gamma t]$, where the *escape-rate* γ is

$$\gamma = D\frac{a}{L^2}, \tag{29}$$

where a is a numerical constant that depends on the geometry of the region of scatterers.

A remarkable fact is that there is also a microscopic expression for the same escape-rate in terms of the dynamical properties of the moving particle in the scattering region. To understand the microscopic formula we need to realize that although the moving particle will eventually escape the region with probability 1, there are an infinite number of possible trajectories for the particle whereby it never leaves the scattering region, i.e., it is never absorbed at the walls. The set of initial positions and velocities of the moving particle, that is, the set of initial points in the phase space of the moving particle, that lead to orbits which are entirely within the scattering region is called the repeller for this system, and we denote it by $\mathcal{R}$. The repeller is typically a fractal set of Lebesgue measure zero in the phase space, but with a non-countable number of points. $\mathcal{R}$ will have a Hausdorff dimension which is slightly less than the dimension of the phase space. The escape-rate γ can be expressed in terms of the dynamical properties of the trajectories that are entirely confined to the repeller as

$$\gamma = \sum_i \lambda_{+,i}(\mathcal{R}) - h_{KS}(\mathcal{R}), \tag{30}$$

where the summation is over all the positive Lyapunov exponents, $\lambda_{+,i}(\mathcal{R})$ for trajectories on the repeller, and $h_{KS}(\mathcal{R})$ is the KS entropy for these trajectories [1,17,32,35]. Note that we have a system for which Pesin's theorem does not hold, but by a small amount of order L^{-2}. To get some feeling for the origin of the escape-rate formula, though by no means a derivation, we return to our argument for the validity of Pesin's theorem [9]. We want to find the rate at which we are obtaining information about the location of the initial points on the repeller. As before, the stretching mechanism provides an exponential rate of information growth about the initial location of the point in phase space, but the probability that the system has not disappeared through the boundary is decreasing exponentially, too. Therefore, we should expect that the rate of information growth for points on the repeller is obtained by combining these two exponential rates as

$$e^{th_{KS}(\mathcal{R})} = e^{[t\sum_i \lambda_{+,i}(\mathcal{R})]}e^{-\gamma t}, \tag{31}$$

or, equivalently, Eq. (30) above. Simple one dimensional maps which illustrate the derivation of the escape-rate formula, and exhibit the structure of the fractal repeller are described in Refs. [1,8,9,36]. As an example the reader might consider the map

$$\begin{aligned} x' &= 3x \quad \text{for} \quad 0 \le x \le 1/2 \\ &= 3x - 2 \quad \text{for} \quad 1/2 < x \le 1 \end{aligned} \tag{32}$$

and suppose that points mapped outside the interval $[0, 1]$ have escaped. For this map the fractal repeller is the middle third Cantor set, the escape rate is $\gamma = \ln(3/2)$, the Lyapunov exponent on the repeller is $\ln 3$, and the KS entropy is $\ln 2$. These results can be understood by realizing that the map stretches all intervals by a factor of 3, accounting for the Lyapunov exponent, and that dynamics on the repeller can be coded by sequences to two symbols, each symbol appearing with equal probability, accounting for the KS entropy on the repeller.

If we now combine the macroscopic expression for the escape-rate, Eq. (29) with the microscopic one, Eq. (30), we obtain an expression for the coefficient of diffusion, D, a transport coefficient, in terms of the dynamical properties of the repeller,

$$D = \lim_{L\to\infty} \frac{L^2}{a} \left[\sum_i \lambda_{+,i}(\mathcal{R}) - h_{KS}(\mathcal{R}) \right], \tag{33}$$

where we have taken the thermodynamic limit to ensure a result that does not contain finite size effects. Eq. (33) is due to Gaspard and Nicolis [17]. Gaspard and Dorfman have extended this method to apply to the other transport coefficients, such as the shear and bulk viscosities, and thermal conductivity of a fluid, as well as for chemical reaction rates [37]. When applying the escape-rate formalism to systems like the Lorentz gas, for example, one usually finds that the Lyapunov exponents and KS entropy for the repeller are equal to their infinite system values plus very small corrections of order L^{-2}. Thus the transport coefficients are contained in these small corrections to the infinite system values, and the transport process is "coded" in the fractal structure of the repeller.

The escape-rate method has been applied to compute the properties of the fractal repeller for a number of model systems, including the multibaker model for diffusion in one

dimensional systems [38], the two dimensional periodic Lorentz gas at sufficiently high density that the free path length of the moving particle is small compared to the dimensions of the system [36,39], to the random Lorentz gas at low densities [40,41], but still with a mean free path small compared to the size of the system, and to Lorentz lattice gases [42]. In these cases the Lyapunov exponents and KS entropies on the repeller differ from their values in the thermodynamic limit, by terms of order L^{-2}. The chief difficulty in using the escape-rate method as a method to compute transport coefficients is that it is as hard or harder to compute the dynamical quantities, particularly $h_{KS}(\mathcal{R})$ as it is to compute the transport coefficient directly, using kinetic theory or other methods. It would be extremely valuable, for example, to have analytic methods to compute $h_{KS}(\mathcal{R})$ directly rather than having to compute γ and $\lambda_{+,i}(\mathcal{R})$ and using the escape rate to obtain the KS entropy on the repeller, as one has to do in the analytic studies of the random Lorentz gas.

B. The Gaussian Thermostat Method

Another way to relate transport coefficients to dynamical quantities, in this case Lyapunov exponents, was developed as a result of efforts to simulate transport processes on the computer using molecular dynamics techniques. It was found early on that the simulations of viscous flow were plagued by the viscous heating of the fluid. To deal with this Evans, Hoover, Nosé, and co-workers developed a thermostatting method that keeps either the kinetic or total energy constant in the fluid undergoing shear [18]. Although the thermostat destroys the symplectic, Hamiltonian structure of the dynamics, we get as compensation, so to speak, a useful and interesting connection between the transport coefficients in the thermostatted system and the Lyapunov exponents for the thermostatted dynamical system, assuming the system approaches a non-equilibrium steady state. The "destruction" of the symplectic structure is something of an overstatement. Liverani and Wojtkowski [43] have shown that these thermostatted systems are conformally symplectic, with useful consequences for the Lyapunov spectrum, and Dettmann and Morriss [44] have shown that the

thermostatted dynamics can be mapped onto Hamiltonian dynamics with unusual canonical position and momentum variables. We refer to their papers for details.

We illustrate the method again for a Lorentz gas with a particle moving among hard disk or sphere scatterers [8,9,45,46]. We suppose that the scatterers are arranged randomly in space or in a regular configuration with a finite free path for the moving particle. We also provide the moving particle with a charge q and suppose that it is acted upon by an external electric field $\vec{E}$, in addition to the scatterers. If there were no thermostat, then the average kinetic energy of the moving particle would increase steadily with time, since the collisions do not affect the kinetic energy, but the field does. To counter this average increase in kinetic energy, we introduce a "thermostat" which keeps the kinetic energy of the moving particle constant between collisions with the scatterers. The equation for the motion of the particle between collisions is given by

$$\begin{aligned} \dot{\vec{r}} &= \vec{p} \\ \dot{\vec{p}} &= \vec{E} - \alpha\vec{p}, \end{aligned} \tag{34}$$

where we have set both the mass, m, and the charge, q, of the moving particle equal to unity. Here α is a function of the momentum and electric field that is fixed by the condition that the kinetic energy be constant, i.e. $\vec{p}\cdot\dot{\vec{p}} = 0$. Thus

$$\alpha = \frac{\vec{E}\cdot\vec{p}}{p^2}. \tag{35}$$

These equations of motion are supplemented by the equations for elastic collisions of the particle with the scatterers,

$$\vec{p}\,' = \vec{p} - 2(\hat{n}\cdot\vec{p})\hat{n}, \tag{36}$$

where $\vec{p}\,'$ is the momentum of the particle after collision, and $\hat{n}$ is a unit vector in the direction from the center of the scatterer to the point of contact with the moving particle at the instant of collision. These equations of motion define a reversible (under $\vec{p}\to-\vec{p}$, $\vec{r}\to\vec{r}$, and $t\to-t$), non-Hamiltonian system in which the phase space volume is not conserved. This latter remark follows from the observation that

$$\frac{\partial \dot{\vec{r}}}{\partial \vec{r}} + \frac{\partial \dot{\vec{p}}}{\partial \vec{p}} = -(d-1)\alpha, \tag{37}$$

where d is the number of spatial dimensions of the system.

These equations have a number of remarkable consequences. Computer simulations show that the system develops a steady state, and that in this steady state the average value of α is positive, $\langle \alpha \rangle_{ss} > 0$, as expected if the thermostat is to keep the system at constant kinetic energy [45,47,48]. Now if the phase space volume is not conserved, but decreases on the average, but the system still settles into a steady state, at least within the resolution of the computer experiment, then it may be heading to a fractal attractor, of lower dimension than the phase space dimension, here, $2d-1$. We will give a simple example of a system that does just this in a moment. Moreover one may define a Gibbs entropy, S_G for this system by

$$S_G = -k_B \int\int d\vec{r} d\vec{p} f(\vec{r}, \vec{p}, t) \left[\ln f(\vec{r}, \vec{p}, t) - 1 \right], \tag{38}$$

where we have assumed the existence of a phase space distribution function, $f(\vec{r}, \vec{p}, t)$, for the moving particle. If this function exists and is differentiable, then it satisfies the conservation equation

$$\frac{\partial f}{\partial t} + \nabla_{\vec{r}} \cdot (f \dot{\vec{r}}) + \nabla_{\vec{p}} \cdot (f \dot{\vec{p}}) = 0. \tag{39}$$

We now use this conservation equation to compute the time rate of change of the Gibbs entropy due to the thermostat [46]. Here we suppose that the Gibbs entropy of the system does not change with time if the thermostat were not present, as is true for systems whose distribution functions satisfy the usual Liouville equation. Now by assuming that the distribution function vanishes at the boundaries (in space and momentum) of the system, we find that

$$\frac{dS_G(t)}{dt} = -k_B \langle \alpha \rangle (d-1), \tag{40}$$

where the angular brackets denote an average with respect to the phase space distribution function f. This result that the entropy decreases with time can be understood, to some

extent, by noting that if the system is heading toward an attractor it is getting localized into a more restricted region of phase space with a concomitant decrease of the Gibbs entropy. The conservation equation, Eq. (39), has yet another consequence of some considerable interest, namely, we express f as $f(\vec{r},\vec{p},t) = 1/V(\vec{r},\vec{p},t)$, where V is the volume of a small phase space region about $(\vec{r},\vec{p})$ where the system is located at time t. Then the equation for f, $\dot{f} = (d-1)\alpha f$, easily obtained from Eqs. (37, 39), leads to

$$\begin{aligned} \frac{d\ln V(t)}{dt} &= -(d-1)\alpha \text{ or} \\ \left\langle \frac{d\ln V(t)}{dt} \right\rangle &= -(d-1) < \alpha > . \end{aligned} \tag{41}$$

Since the rate of change of small volume elements in phase space is governed by the sum of the Lyapunov exponents,

$$V(\vec{r},\vec{p},t) \sim \exp\left[t \sum_i \lambda_i(\vec{r},\vec{p}) \right], \tag{42}$$

where we may imagine that the Lyapunov exponents depend upon the phase space point, and the sum is over *all* of the exponents, not just the positive ones. From this it follows that

$$(d-1)\,\langle\alpha\rangle = -\left\langle \sum_i \lambda_i(\vec{r},\vec{p}) \right\rangle. \tag{43}$$

Therefore, we can relate the average friction coefficient to the average value of the sum of the Lyapunov exponents [18].

We now push this analysis into the realm of transport theory by returning to the calculation of the rate of change of the Gibbs entropy. In a non-equilibrium steady state, the rate of decrease of the Gibbs entropy must be at least matched by an increase in entropy of the heat reservoir that is removing the heat generated by the dynamical processes in the system. If we identify this positive rate of entropy production with the irreversible entropy production required by irreversible thermodynamics $\sigma E^2/k_B T$, where σ is the coefficient of electrical conductivity, T is the thermodynamic temperature, and k_B is Boltzmann's constant, we find that

$$\sigma = -\frac{k_B T}{E^2} \left\langle \sum_i \lambda_i \right\rangle. \tag{44}$$

Eq. (44) is the main result of this analysis [18]. It shows that a transport coefficient, in this case the electrical conductivity, is proportional to the average rate of phase space contraction as measured by the sum of all of the Lyapunov exponents. We will comment in the final section upon the obviously problematic issues concerning the use of entropy production arguments here.

For small fields the electrical conductivity of the moving particle and its diffusion coefficient in the Lorentz gas are directly related by a simple factor, $D = [(p^2/(q^2 m)]\sigma$, and Eq. (44) then provides another expression for the diffusion coefficient in terms of dynamical quantities, the sum of all of the Lyapunov exponents of the system. Similar expressions can be obtained for other transport coefficients. The coefficient of shear viscosity, in particular has been studied in great detail for particles that interact with short ranged repulsive potentials, i.e. WCA particles [18,49].

The evaluation of these expressions for transport coefficients appears to be formidable since one has to determine the complete Lyapunov spectrum for the thermostatted system in an external field. This situation has been simplified to a great extent by the observation, and in some cases the proof [43,49,50], of a *conjugate pairing rule* for these thermostatted systems. That is, the non-zero Lyapunov exponents can be ordered in conjugate pairs, λ_i, λ_{-i}, say, such that the sum of each conjugate pair is the same for all conjugate pairs. Consequently, the sum of all of the Lyapunov exponents is equal to the product of the number of conjugate pairs and the sum of one conjugate pair. This is of course a generalization of the conjugate pairing rule for symplectic systems, where the sum is zero. The conjugate pairing rule for thermostatted systems has been observed in computer simulations, and has been proved analytically for a number of systems, provided the thermostat keeps the total kinetic energy [43,50], rather than the total energy, kinetic plus potential, constant. Of course for hard sphere type systems, there is no difference between the kinetic and total energies.

C. A Simple Map with an Attractor

In order to see how a fractal attractor might form in the phase space for a thermostatted system we turn once again to a simple two dimensional map. Here we construct a map that has some of the features that we expect to see in a thermostatted Lorentz gas, for example. That is, we consider a map with reversible, hyperbolic dynamics, but allow for a phase space volume contraction in part of the phase space. Such a map is provided by a map Φ of the unit square onto itself given by

$$\begin{aligned} \Phi(x,y) &= (x/l, ry) \quad \text{for} \quad 0 \le x \le l \\ &= ((x-l)/r, r+ly)) \quad \text{for} \quad l < x \le 1, \end{aligned} \tag{45}$$

where $l, r > 0, l \neq r$, and $l + r = 1$. This map is illustrated in Fig. 8. One can easily calculate the positive and negative Lyapunov exponents for this map and they are

$$\lambda_+ = l \ln \frac{1}{l} + r \ln \frac{1}{r}, \tag{46}$$

$$\lambda_- = l \ln r + r \ln l, \text{ and} \tag{47}$$

$$\lambda_+ + \lambda_- = (l - r) \ln \frac{r}{l} \le 0. \tag{48}$$

Here the equality holds in the last equation only if $l = r = 1/2$. The SRB theorem tells us that the time average of any continuous function defined on the unit square will approach an ensemble average taken with respect to the appropriate SRB measure. Some reflection will convince the reader that the SRB measure is smooth in the expanding, or x, direction but fractal in the contracting, or y, direction. The details of this and related SRB measures are described in Ref. [51]. We say that the system has evolved to a fractal attractor with a smooth measure in the x direction and fractal in the y direction. This attractor is invariant under the map Φ since the limiting form of the set is not changed by the map, or for that matter its inverse, Φ^{-1} which can easily be constructed. Another interesting point about this map Φ is related to its reversibility property. The map Φ^{-1} has exactly the same Lyapunov exponents as the map Φ. However the SRB measure for the inverse map is smooth in the expanding y direction but fractal in the contracting x direction, and the time reversed

attractor is also invariant under the two maps, Φ and its inverse. Sometimes we call this pair of invariant sets an attractor with a corresponding repeller. Depending on the direction of the time, one of the two invariant sets is an attractor, and the other is a repeller.

D. Fractal Forms for Diffusion Coefficients

Our discussions in this section have been largely formal. To conclude this section, we will consider the case of deterministic diffusion in one dimension under the action of a simple, piecewise linear map, such as that illustrated in Fig. 9. This map has the general form $x_{n+1} = M(x_n)$, where $M(x)$ is a piecewise linear function of x, and satisfies the condition $M(x+1) = 1 + M(x)$. In the interval $0 \leq x \leq 1$, $M(x)$ is given explicitly by

$$\begin{aligned} M(x) &= ax \qquad \text{for} \quad 0 \leq x \leq 1/2 \\ &= ax + (1-a) \quad \text{for} \quad 1/2 < x \leq 1, \end{aligned} \tag{49}$$

where the slope of the map a satisfies the condition $a > 2$, which is necessary for diffusion to take place at all. R. Klages studied this and similar maps for his Ph. D. work [52]. The diffusion coefficient could be obtained by mapping this system onto a Markov process using a one dimensional version of Markov partitions. All of the appropriate details are given in Klages' dissertation and in Refs. [53,54]. Here we will consider the shape of the diffusion coefficient, D, as a function of the slope a for $a > 2$. The values of D for even integer a can easily be found by mapping this process onto a simple random walk on a line with a non zero probability, depending on a, of staying at the same site. For odd integer a, the problem is not much harder and D can also be obtained easily. The method of Markov partitions gives D for a dense set of values of a on the real line, and this is used to give the general structure of the dependence of D upon a. This dependence is illustrated in Fig. 10. There we see that D is a fractal function of a with quite a rich fractal structure. This rather surprising structure shows that transport coefficients are not always simple functions of the parameters of the system. Further studies on models of this type are underway by Klages [55] and by J. Groeneveld [56].

We have established some interesting relations between dynamical and transport quantities and showed that fractal structures in the microscopic phase space have properties that are directly related to macroscopic transport properties of the system. In the next section we look at questions of the dynamical foundations of irreversible kinetic equations and show how such equations can be used to compute, among other things, Lyapunov exponents and KS entropies, for the Lorentz gas, as an example.

IV. THE DYNAMICAL FOUNDATIONS OF KINETIC EQUATIONS

Two ideas have been developed in the previous sections which seem to be central to an understanding of the dynamical origins of irreversible phenomena in fluids. In particular, we can now isolate some of the key features that must be taken into account when one tries to understand the efficacy of stochastic equations such as the Boltzmann transport equation for describing irreversible processes in gases. Briefly stated, these two central ideas are:

(1) One can, for Anosov systems and probably with suitable modifications for hard sphere systems as well, separate the tangent space at a particular point in phase space and, in fact, phase space itself, into expanding, contracting and center manifolds. The expanding and contracting manifolds exchange behavior on the time reversed motion.

(2) Measures tend to be smooth in the unstable, or expanding, directions, and fractal in the stable, or contracting, directions.

Therefore one can imagine the following scenario for the derivation of an irreversible equation from a dynamical analysis. Consider some initial ensemble distribution in phase space that is a measureable function of the phase space variables with respect to the microcanonical measure, say. To be specific consider an initial distribution which is unity on a certain set A of small measure and zero elsewhere. In the course of time, this set will be stretched along the unstable directions, becoming more and more uniformly distributed in these directions, but forming more and more of a fractal structure in the stable directions. If then, we project the distribution function onto the unstable directions, say by integrating

over the stable directions and thereby obtaining a reduced distribution function, we ought to see the approach to a uniform distribution function in the projected variables.

To make this argument less abstract and more transparent, we consider its application to our familiar models, the baker map [8,57,58] and the Arnold cat map. To begin we will need the version of Liouville's equation appropriate for maps that that evolve at discrete time intervals, called the Perron-Frobenius equation [1,30].

A. The Perron-Frobenius Equation

We consider a map of some region R onto itself. To be definite we take R to be two dimensional, and the map to be of the form

$$(x', y') = \Phi(x, y) = (\Phi_1(x, y), \Phi_2(x, y)). \tag{50}$$

We consider R to be our phase space, and we suppose there is some phase space distribution evolving from some initial distribution on R denoted by $\rho_0(x, y)$. Then after n iterations of the map, a new distribution function, $\rho_n(x, y)$, is obtained which satisfies the recursion equation

$$\rho_n(x, y) = \int_R \int dx' dy' \delta(x - \Phi_1(x', y'))\delta(y - \Phi_2(x', y')) \cdot \rho_{n-1}(x', y'). \tag{51}$$

This recursion equation, the Perron-Frobenius equation, is self-evident provided the delta functions are not to be evaluated at possible discontinuity points of the distribution function. The delta functions can be evaluated in terms of the pre-image points of (x, y), and the Jacobian of the map Φ at these pre-image points. The examples to which we apply this equation are simple area preserving maps on the unit square for which the Jacobian of Φ is simply unity, but more general cases can be treated as well.

B. The Baker's Map

To apply the Perron-Frobenius equation to the baker's map, we take R to be the unit square, and the mapping Φ to be given by Eq. (5). An elementary calculation leads to the recursion equation

$$\begin{aligned} \rho_n(x,y) &= \rho_{n-1}(x/2,2y) \quad \text{for} \quad 0 \le y < 1/2 \\ &= \rho_{n-1}(\tfrac{x+1}{2},2y-1) \quad \text{for} \quad 1/2 \le y \le 1. \end{aligned} \tag{52}$$

For this map the unstable direction is the x-direction, and we can define a reduced distribution function that only depends on x by integrating over the y variation of $\rho_n(x,y)$. We therefore define $W_n(x)$ by

$$\begin{aligned} W_n(x) &= \int_0^1 dy \rho_n(x,y) \\ &= \int_0^{1/2} dy \rho_{n-1}(x/2,2y) + \int_{1/2}^1 dy \rho_{n-1}(\frac{x+1}{2},2y-1) \\ &= \frac{1}{2}\left[W_{n-1}(\frac{x}{2}) + W_{n-1}(\frac{x+1}{2})\right] \end{aligned} \tag{53}$$

This equation can be considered to be a model "kinetic" equation since it is obtained from the discrete form of Liouville's equation by integrating over the y variation. The reader may also notice that Eq. (53) is itself the Perron-Frobenius equation for the map $x' = 2x \bmod 1$. It is easy to see that $W_n = 1$, or any non-zero constant, is a solution of this equation, and we require that ρ_n and W_n be non-negative so that they can represent probability distributions. Moreover there is an H-theorem associated with Eq. (53), very similar to Boltzmann's H-theorem. That is, we define $H_n = \int_0^1 dx W_n(x) \ln W_n(x)$, and elementary inequalities based upon the observation that a straight line connecting two points on the curve $z = u \ln u$ lies below the curve show that $H_n \le H_{n-1}$. The equality sign holds only if W_n is a constant. Finally, Eq. (53) can be solved if $W_0(x)$ is a measurable function of x, and any arbitrary, normalized initial distribution will approach 1 as $n \to \infty$. It is important to note that we have done nothing more than integrate the Perron-Frobenius equation for this map over the coordinate in the stable direction, assuming only that the initial distribution

function is well behaved. As the time increases, the reduced distribution function becomes an increasingly smoother function of x, finally reaching an equilibrium distribution, in a monotonic, irreversible manner. Now if we were to start with the same initial distribution function $\rho_0(x, y)$, but follow the time reversed map, then the unstable direction is parallel to the y axis, and the reduced distribution function would be obtained by integrating the Perron-Frobenius equation for the time reversed motion over x. The resulting equation would be identical to Eq. (53), with x replaced by y. The reversibility of the underlying equations of motion is still preserved but irreversible equations are obtained by selecting the direction of time and projecting the full distribution function onto the unstable manifold. The reader is also invited to see what happens if the distribution function is projected onto the stable manifold, for the baker's map. The paper by Tasaki and Gaspard [59] should prove useful for this analysis.

C. The Arnold Cat Map

As an extension of the ideas just discussed we consider now the Arnold cat map. The analysis of the corresponding Perron-Frobenius equation is complicated by the fact that the unstable and stable directions are not oriented along the x and y axes respectively, but are rotated by a fixed angle. Instead of working out the mathematics let us just look at the map on the computer. We will be interested in the reduced distributions projected onto the x-axis or onto the y-axis. This is a little closer to what we need to understand the Boltzmann equation since for a dilute gas with N particles we do not know the directions of the stable and unstable manifolds in phase space, but we do consider a projected or reduced distribution function, namely the single particle distribution function obtained by integrating the Liouville distribution over the phases of all but one particle.

We start with the same initial distribution function for the Arnold cat map as illustrated in Fig. 4, that is, where all of the distribution is concentrated in the lower left corner of the unit square. In Fig. 11 we plot the distribution function projected onto the x-axis, for

various times starting with a step function at $t = 0$. Note that this function also becomes smooth with time and appears to have reached equilibrium after four steps. Now consider the same map but project the distribution function onto the y-axis. this is illustrated in Fig. 12. Exactly the same things happen. This reduced distribution function also approaches an equilibrium value after a ten time steps or so. One can also show that H-functions defined in terms of either of these distribution functions decrease monotonically in time. If one reverses the motion, then very similar things will happen: both of the reduced distribution functions, whether projected on the x or y axes will approach equilibrium. Only if we project somehow onto the stable direction will we not see an evolution to a smooth equilibrium distribution.

We conclude from a study of these maps that the approach of a reduced distribution function to a smooth equilibrium value depends only on the construction of a reduced distribution function that is obtained by projecting the full distribution function onto a direction that is not orthogonal to unstable directions in phase space. Of course this is really a conjecture. It is an important and open problem to work this out in detail for more realistic systems. Furthermore, we might be asking too much of realistic systems that this picture be realized in essence for them. Instead only much weaker properties may really be necessary for the variables of physical interest, such as the pressure exerted by a gas on the walls of the container, to show an approach to equilibrium. However, for Anosov systems, at least, where there is a very clear decomposition of the entire phase space into stable, unstable, and center manifolds, the picture sketched above is likely to hold.

D. The Random Lorentz Gas

In this subsection we briefly indicate how the Boltzmann equation itself may be used to calculate the Lyapunov exponents of a simple model of a gas, the hard disk Lorentz model [40,41,47]. To do this we combine the ideas of Boltzmann with those of Ya. G. Sinai [15], thereby suggesting the existence of a deep connection between "molecular chaos"- the stochastic hypothesis that underlies the Boltzmann transport equation- and dynamical

chaos, which shows that stochastic-like behavior is possible even for deterministic mechanical systems.

Consider a collection of hard disks of radius a placed at random on a plane with number density n, such that $na^2 << 1$. The moving particle always travels with the same speed, v and makes elastic collisions with the scatterers. To calculate the Lyapunov exponent we consider two trajectories on the constant energy surface that are infinitesimally close to each other, but separating, nonetheless. We consider the separation of a diverging bundle of trajectories in position space, since if this separation grows exponentially, so will the separation in velocity space, since both have to grow with the same exponential. We suupose without loss of generality that if we follow the trajectory bundle backward in time all the trajectories go through a common point of intersection. The separation of two trajectories in the bundle can be expressed in terms of a radius of curvature, ρ, which is the distance from the present position of the trajectories to the point of intersection. If we denote the distance between the two trajectories by Δ, one finds that (see Fig. 13)

$$\frac{d\Delta}{dt} = \frac{v\Delta}{\rho} \tag{54}$$

This equation has the simple solution

$$\Delta(t) = \exp\left(\int_0^t d\tau \frac{v}{\rho(\tau)}\right)\Delta(0). \tag{55}$$

It now follows immediately, from the fact that this system is ergodic that the positive Lyapunov exponent, λ_+, is given as

$$\lambda_+ = v\left\langle \frac{1}{\rho} \right\rangle, \tag{56}$$

where the brackets denote an ensemble average. Therefore we need to determine the ensemble distribution for the radius of curvature. This is the point where the Boltzmann equation becomes useful. Let us consider an "extended" distribution function, $F(\vec{r}, \vec{v}, \rho, t)$, which includes the position of the moving particle, $\vec{r}$, its velocity, $\vec{v}$ the time, t, and the radius of curvature, ρ, as variables. In a sense this is a two particle distribution function since the

separation of two trajectories is included as one of the variables. Now we know how $\vec{r}$ and $\vec{v}$ change during free motion and at a collision with a scatterer. The radius of curvature ρ grows linearly with time during the free motion as $\rho(t+dt) = \rho(t) + v\,dt$, and changes from a precollision value ρ^- to a post collision value ρ^+ at a collision, where

$$\frac{1}{\rho^+} = \frac{1}{\rho^-} + \frac{2}{a\cos\phi}, \tag{57}$$

where ϕ is the angle of incidence at collision [15]. Typically ρ^- is on the order of the mean free path between collisions, and ρ^+ is always less than or equal to $a/2$.

Using standard methods of kinetic theory one can derive the following equation for $F(\vec{r},\vec{v},\rho,t)$, the extended Lorentz-Boltzmann equation

$$\left[\frac{\partial}{\partial t} + \vec{v}\cdot\nabla + v\frac{\partial}{\partial\rho}\right] F(\vec{r},\vec{v},\rho,t) = -\nu F(\vec{r},\vec{v},\rho,t)$$
$$+(\nu/2)\int_{-\pi/2}^{\pi/2} d\phi \int_0^\infty d\rho' \cos\phi\,\delta\left(\rho - \frac{(a\cos\phi)/2}{1+(a\cos\phi)/(2\rho')}\right)$$
$$\times F(\vec{r},\vec{v}',\rho',t), \tag{58}$$

and $\vec{v}' = \vec{v} - 2(\hat{n}\cdot\vec{v})\hat{n}$, as in Eq. (36), and $\nu = 2nav$ is the average collision frequency for the moving particle. This equation can be solved easily for an equilibrium system where F does not depend on $\vec{r}$ or t. The details of the derivation and the solution are given elsewhere [9], but here we give the final result

$$\lambda^+ = 2nav(1 - C - \ln(2na^2)), \tag{59}$$

where C is Euler's constant. We emphasize the point that not only does dynamical systems theory allow us to understand, to some extent at least, the dynamical origins of kinetic theory, kinetic theory in turn can be used to compute important quantities needed to show that the ideas we have been discussing are indeed relevant for our understanding of irreversible processes in fluids.

V. CONCLUSIONS

Our excursion into the dynamical foundations of the kinetic theory of gases has provided us with a very stimulating and suggestive picture of irreversible processes. If we can show that a typical system like a gas of hard spheres or WCA particles is indeed an Anosov system, then many striking consequences are immediate. In particular, the phase space has a tangent space almost everywhere which can be decomposed into unstable, stable, and neutral subspaces. Measures and distribution functions become smooth with time along the unstable directions, approaching equilibrium values as the time gets very large compared to characteristic microscopic times. The reversibility of the equations of motion reflects itself in the interchange of stable and unstable directions under time reversal, so that equilibrium states appear in the time reversed motion as the distribution function becomes smooth along the unstable directions of the time reversed motion.

If this picture is correct then we can relate microscopic dynamical quantities such as Lyapunov exponents and KS entropies to macroscopic quantities such as transport coefficients, Here we illustrated this connection using the escape-rate formalism, and the method of Gaussian thermostats. However, these are only two of a number of useful methods for making this connection. For example, methods based on periodic orbit expansion or Ruelle-Pollicott resonances are under very active study at the present time [5,60].

We conclude with a few remarks:

1) We have presented a picture here of how things might be for a typical system of interest to those applying kinetic theory methods to compute transport properties. It is not known whether this picture is indeed correct. We must study a number of systems of increasingly more realistic structures in order to get deeper insights into this question. Progress is being made in this direction using both computer and analytical studies of a number of different systems.

2) We know very little about the complicated fractal structures that underlie transport processes in fluids, i.e., the attractors and repellers that we have discussed earlier. Only

for simple two dimensional maps do we have any good intuition about these fractals. Even higher dimensional maps would provide useful examples for more complicated systems.

3) We have not mentioned many aspects of dynamical systems theory that are relevant for a further analysis of the topics discussed here. In particular, the thermodynamic formalism of Sinai, Bowen and Ruelle [14,61] provides a close, but often very formal, connection between dynamical systems theory and equilibrium statistical mechanics. This connection is surely not accidental, and can be very helpful for understanding the dynamical foundations of statistical mechanics, in general.

4) The reader may have been surprised by the appearance of a negative entropy production in the discussion of the Gaussian thermostatted systems in Sec. 3.2. This negative sign is really not mysterious, since we are gaining more information about the system as its phase space trajectory becomes more and more localized on an attractor. In equilibrium thermodynamics one can reduce the entropy of a gas by applying work in a reversible, isothermal compression. However, the entropy of the universe stays constant when one takes into account the entropy change of the thermostat that works on the gas. Here, similarly, one has to consider the system *plus* the thermostat in order to make sense of the entropy production. In a steady state the total entropy production must be zero, so the negative entropy production of the system must be matched by a positive entropy production in the thermostat.

A number of papers have been written recently which discuss this topic in more detail. Ruelle has proved that the entropy production by the thermostat must be strictly positive [62]. Tel, Vollmar and Breymann have discussed the entropy production for a simple model based upon the baker map from the point of view of coarse graining the phase space [63,64]. Here the point is that we are unable, experimentally, to follow the localization of the thermostattes system onto the attractor because we are limited to the resolution of our observing devices. Therefore beyond a certain point we will not see the entropy of the thermostatted system decrease. Instead we will see the entropy of the coarse grained, observed, system increase as the microscopic processes take place on a scale that is too fine for our measuring

devices. In the Tel, Vollmer, and Breymann analysis the positive entropy production is taken to be the difference between the information available in a coarse grained description where nothing is changing beyond a certain scale and the information available in a complete microscopic description where one can follow the trajectory onto the attractor. There still needs to be a study where one connects this idea of coarse graining to a physical description of a thermostat and shows that including the entropy production in the thermostat is equivalent to coarse graining the phase space of the thermostatted system.

5) P. Gaspard has discussed entropy production for a simple reversible system which consists of a chain of baker's maps coupled in such a way that a density gradient may be established and maintained. He shows that the positive entropy production associated with this process is connected to the fractal structure that develops in the system as the steady density gradient is established. The phase space density is not a differentiable function of the phase space variables, and one can only define a coarse grained entropy for the system. Gaspard shows that this coarse grained entropy is positive an its production has the form required by irreversible thermodynamics.

6) We have not mentioned quantum mechanics at all. It seems inconsistent with our physical understanding of matter to restrict our attention exclusively to classical systems. The quantum versions of the ideas discussed here are still in the early phases of development and we refer the reader to the literature for further details [66]. This is an area where even our understanding of even the simplest systems is not entirely secure.

To conclude, there is a lot of work still to do in order to undertand in detail the chaotic foundations of transport theory and to provide a clear microscopic explanation of all of the phenomena that we associate with irreversible processes in fluids.

ACKNOWLEDGEMENTS: The author would like to thank Henk van Beijeren, E. G. D. Cohen, Matthieu Ernst, Pierre Gaspard, Edward Ott, and Tamas Tel for many helpful conversations as well as Thomas Gilbert for many helpful discussions on SRB measures. He would like to thank Charles Ferguson and Rainer Klages for supplying a number of the figures, and he would also like to thank them as well as Thomas Gilbert, Luis Nasser, and

Debabrata Panja for many helpful and clarifying discussions, and especially Ramses van Zon for a critical reading of this manuscript. He thanks the National Science Foundation for support under Grant PHY-96-00428.

---

[1] E. Ott, *Chaos in Dynamical Systems*, Cambridge University Press, Cambridge, (1992).

[2] H. Poincaré, *New Methods in Celestial Mechanics*, D. L. Goroff, Ed., A. I. P. Press, New York, (1993).

[3] J. Lebowitz and O. Penrose, Physics Today **26**, 23, (1973).

[4] J.-P. Eckmann, and D. Ruelle, Rev. Mod. Phys. **57**, 617, (1985).

[5] P. Gaspard, *Chaos, Scattering, and Statistical Mechanics*, Cambridge University Press, Cambridge, (to appear).

[6] J.Guckenheimer and P. Holmes, *Nonlinear Oscillations, Dynamical Systems, and Bifurcations of Vector Fields*, Springer Verlag, Berlin, (1983).

[7] K. T. Alligood, T. D. Sauer, and J. A. Yorke, *Chaos: An Introduction to Chaotic Systems*, Springer Verlag, new York, (1997).

[8] J. R. Dorfman, *From Molecular Chaos to Dynamical Chaos*, Lecture Notes, University of Utrecht, and University of Maryland, College Park, (1997).

[9] J. R. Dorfman and H. van Beijeren, Physica A**240**, 12, (1997).

[10] J. R. Dorfman and H. van Beijeren, in B. Berne (Ed.), *Statistical Mechanics, B*, Plenum Press, New York, (1977).

[11] P. Resibois and M. deLeener, *Classical Kinetic Theory of Fluids*, Wiley, New York, (1977).

[12] S. Chapman and T. G. Cowling, *The Mathematical Theory of Non-Uniform Gases*, 3rd. Ed.,

Cambridge University Press, Cambridge, (1970).

[13] R. Bowen, *Equilibrium States and the Ergodic Theory of Anosov Diffeomorphisms*, Lecture Notes in Mathematics, No. 470, Springer Verlag, Berlin, (1975); *On Axiom A Diffeomorphisms*, Regional Conference Series in Mathematics, No. 35, American Mathematical society, Providence, (1978); R. Bowen and D. Ruelle, Invent. Math. **29**, 181, (1975).

[14] D. Ruelle, *Thermodynamic Formalism*, Addison-Wesley, Reading Ma., (1978); Am. J. Math., **98**, 619, (1976); Phys. Math. IHES, **50**, 275, (1979); *Elements of Differentiable Dynamics and Bifurcation Theory*, Academic Press, New York, (1989); D. Ruelle and Ya. G. Sinai, Physica A**140**, 1, (1986).

[15] Ya. G. Sinai, *Introduction to Ergodic Theory*, Princeton University Press, Princeton, (1976); Russ. Math. Surv. **25**, 137, (1970); *Dynamical Systems*, World Scientific, Singapore, (1991); Russ. Math. Surv., **21**, 21, (1972); *Topics in Ergodic Theory*, Princeton University Press, Princeton, (1994).

[16] A. Katok and B. Hasselblatt, *Introduction to the Modern Theory of Dynamical Systems*, Cambridge University Press, Cambridge, (1995).

[17] P. Gaspard and G. Nicolis, Phys. Rev. Lett., **65**, 1693, (1990).

[18] D. J. Evans and G. P. Morriss, *Statistical Mechanics of Nonequilibrium Liquids*, Academic Press, London, (1990); W. G. Hoover, *Computational Statistical Mechanics*, Elsevier, Amsterdam, (1991). See also papers collected in M. Mareschal and B. Holian, (Eds.), *Microscopic Simulations of Complex Hydrodynamic Phenomena*, Plenum Press, New York, (1992).

[19] G. E. Uhlenbeck and G. W. Ford, *Lectures in Statistical Mechanics*, American Mathematical Society, Providence, (1963).

[20] V. I. Arnold and A. Avez, *Ergodic Problems of Classical Mechanics*, Benjamin, New York, (1968).

[21] G. D. Birkhoff, Proc. Nat. Acad. Sci. **17**, 656, (1931).

[22] D. Szasz, Stud. Scient. Math. Hungarica, **31**, 299, (1996); Physica A**194**, 86, (1993).

[23] N. Simanyi and D. Szasz, "Ergodicity of Hard Spheres in a Box", (to be published).

[24] C. Liverani and M. Wojtkowski, "Ergodicity in Hamiltonian Systems" in *Dynamics Reported (New Series)*, Vol 4. Springer Verlag, Berlin (1995), p. 130.

[25] G. Gallavotti and D. Ornstein, Comm. Math. Phys., **38**, 83, (1974).

[26] Ya. G. Sinai, Funct. Anal. Appl. **13**, 192, (1980).

[27] K. Peterson, *Ergodic Theory*, Cambridge University Press, Cambridge, (1983).

[28] P. Billingsley, *Ergodic Theory and Information*, Wiley, New York, (1965).

[29] V. I. Arnold, *Mathematical Methods in Classical Mechanics*, 2nd. Ed., Springer Verlag, Berlin, (1989).

[30] A. Lasota and M. C. Mackey, *Chaos, Fractals, and Noise* 2nd. ed. Springer Verlag, Berlin, (1994).

[31] Ya. Pesin, Russ. Math. Surv. **32**, 55, (1997).

[32] P. Gaspard and J. R. Dorfman, Phys. Rev. E**52**, 3525, (1995).

[33] O. E. Lanford in *Chaotic Behavior of Deterministic Systems*, G. Iooss, R. H. G. Helleman and R. Stora, Eds., North Holland, Amsterdam, (1983), p. 6.

[34] G. Gallavotti and E. G. D. Cohen, J. Stat. Phys. **80**, 931, (1995).

[35] T. Tel in *Directions in Chaos*, Vol. 3, Hao Bai-Lin, Ed., World Scientific, Singapore, (1990).

[36] P. Gaspard and F. Baras, in M. Mareschal and B. Holian, (Eds.), *Microscopic Simulations of Complex Hydrodynamic Phenomena*, Plenum Press, New York, (1992), p. 301.

[37] J. R. Dorfman and P. Gaspard, Phys. Rev. E**51**, 28, (1995).

[38] P. Gaspard, J. Stat. Phys. **68**, 673, (1992).

[39] P. Gaspard and F. Baras, Phys. Rev. E**51**, 5332, (1995).

[40] H. van Beijeren and J. R. Dorfman, Phys. Rev. Lett.,**74**, 4412, (1995); **76**, 3238(E), (1996).

[41] A. Latz, H. van Beijeren, and J. R. Dorfman, Phys. Rev. Lett. **78**, 207, (1997).

[42] M. H. Ernst, J. R. Dorfman, R. Nix, and D. Jacobs, Phys. Rev. Lett. **74**, 4416, (1995).

[43] M. P. Wojtkowski and C. Liverani, "Conformally Symplectic Dynamics and Symmetry of the Lyapunov Spectrum", preprint, (1997)

[44] C. P. Dettmann and G. P. Morriss, Phys. Rev. E**54**, 2495, (1996); **55**, 3693, (1997).

[45] G. P. Morriss, C. P. Dettmann, and L. Rondoni, Physica A**240**, 84, (1997); J. P. Lloyd, M. Niemeyer, L. Rondoni, and G. P. Morriss, Chaos, **5**, 536, (1995).

[46] N. I. Chernov, G. I. Eyink, J. L. Lebowitz, and Ya. G. Sinai, Comm. Math. Phys. **154**, 569, (1993).

[47] H. van Beijeren, J. R. Dorfman, E. G. D. Cohen, Ch. Dellago, and H. A. Posch, Phys. Rev. Lett. **77**, 1974, (1996).

[48] Ch. Dellago, H. A. Posch, and W. G. Hoover, Phys. Rev. E**53**, 1485, (1996).

[49] D. J. Evans, E. G. D. Cohen, and G. P. Morriss, Phys Rev. A**42**, 5990, (1990).

[50] C. P. Dettmann and G. P. Morriss, Phys. Rev. E**53**, R5541, (1996).

[51] S. Tasaki (private communication and to be published).

[52] R. Klages *Deterministic Diffusion in One-Dimensional Maps* Ph. D. Dissertation, Technical University of Berlin, Berlin, (1995).

[53] R. Klages and J. R. Dorfman, Phys. Rev. Lett. **74**, 387, (1995).

[54] R. Klages and J. R. Dorfman, Phys. Rev. E**55**, R1247, (1997).

[55] R. Klages (unpublished)

[56] J. Groenveld (unpublished)

[57] M. V. Berry, in S. Jorna, (Ed.), *Topics in Nonlinear Dynamics*, A. I. P. conference Proceedings, No. 46, American Institute of Physics, New York, (1978).

[58] L. Reichl, *A Modern Course in Statistical Mechanics*, University of Texas Press, Austin, (1980).

[59] S. Tasaki and P. Gaspard, J. Stat. Phys. **81**, 935, (1995).

[60] P. Gaspard, Phys. Rev. E**53**, 4379, (1996).

[61] C. Beck and F. Schlögl, *Thermodynamics of Chaotic Systems*, Cambridge University Press, Cambridge, (1993).

[62] D. Ruelle, J. Stat Phys. **85**, 1, (1996).

[63] T. Tel, J. Vollmer, and W. Breymann, Europhys. Lett. **35**, 659, (1996); Phys. Rev. Lett. **77**, 2945, (1996).

[64] G. P. Morriss and L. Rondoni, Physica A**233**, 767, (1996).

[65] P. Gaspard, Physica A**240**, 54, (1997); J. Stat. Phys. (to appear).

[66] G. Casati and B. Chirikov (Eds.), *Quantum Chaos*, Cambridge University Press, Cambridge, (1995); K. Nakamura, *Quantum Chaos*, Cambridge University Press, Cambridge, (1994); see also CHAOS, **3**, No. 4, (1993).

FIGURE CAPTIONS

Figure 1. The tent map on the unit interval $0 \leq x \leq 1$.

Figure 2. The baker's map on the unit square $0 \leq x, y \leq 1$.

Figure 3. The Arnold cat map on the unit square.

Figure 4. The initial set A is confined to the lower left corner of the unit square. The dynamics of the points in this set is governed by the Arnold cat map.

Figure 5. The evolution of the set A after 2 iterations of the Arnold cat map.

Figure 6. The evolution of the set A after 3 iterations of the map.

Figure 7. The evolution of the set A after 10 iterations. The initial set A consisted of 10^5 points, and the continuous nature of the initial set is no longer preserved. With more points, this evolved set would appear to be a set of closely spaced parallel lines, nearly convering the unit square uniformly.

Figure 8. A simple map on the unit square with an attractor. The map is given by Eq. (45), and the areas of regions I and II individually are not preserved by the map.

Figure 9. The one-dimensional piecewise linear map given by Eq. (49). Here $a > 2$.

Figure 10. The diffusion coefficient D as a function of the slope of the map a, for the map in Figure 9. Curve (a) is the function over the range $2 \leq a \leq 8$. Curves (b)-(f) show the diffusion coefficient at various magnifications. The error bars are too small to be noticeable on these graphs.

Figure 11. The x-distribution function for the Arnold cat map at iterations $n = 0, 1, 2, 3, 4$, showing that the distribution becomes nearly uniform after 4 iterations. The initial condition is the same as in Figure 4. These curves are affected by a small computer

generated error.

Figure 12. The y-distribution function for the Arnold cat map at the same iterations as in Figure 11, for the same initial conditions.

Figure 13. The growth of the radius of curvature between collisions.

Figure 14. The change in the radius of curvature at collision.

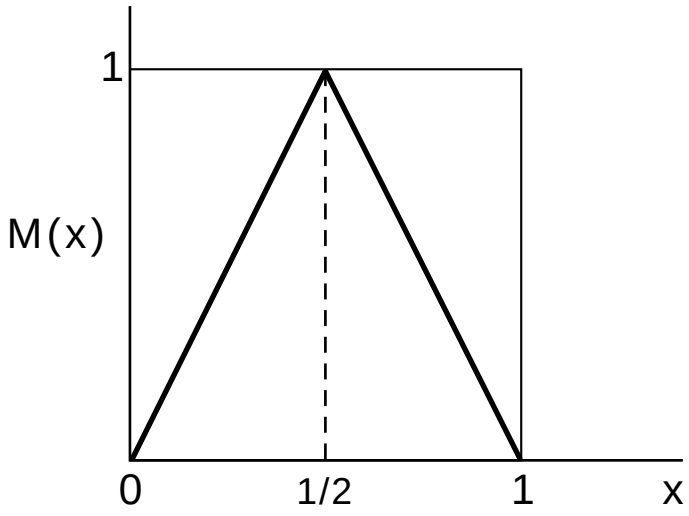
1
M(x)
0
1/2
1
x

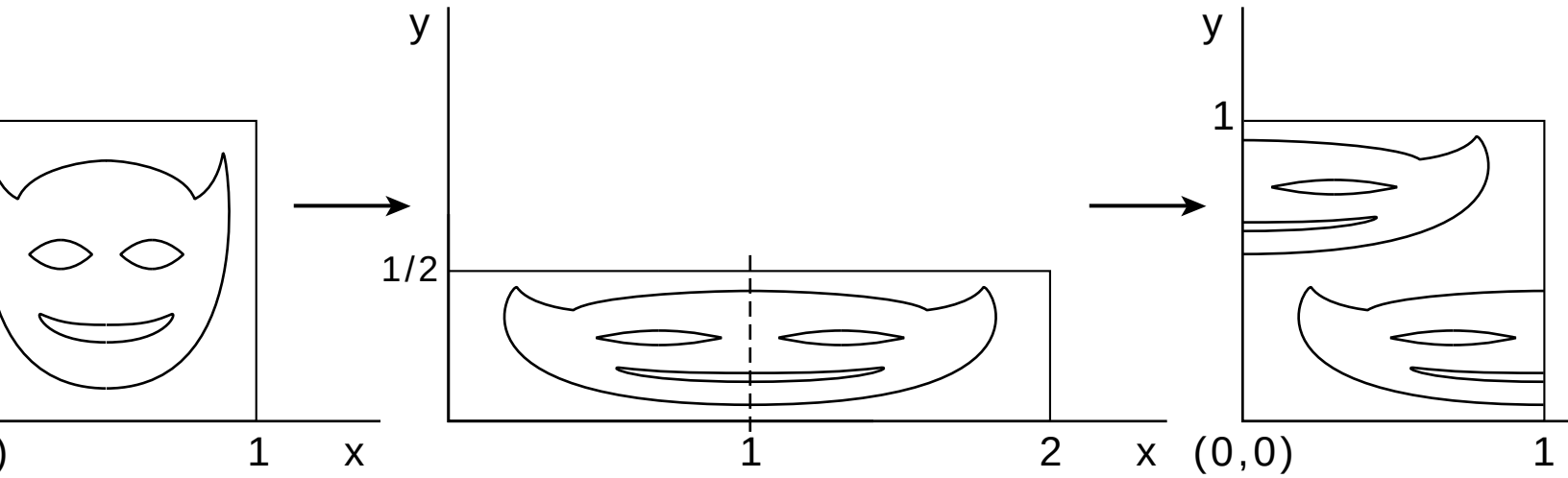
y
1/2
1
2
x
y
1
(0,0)
1
x

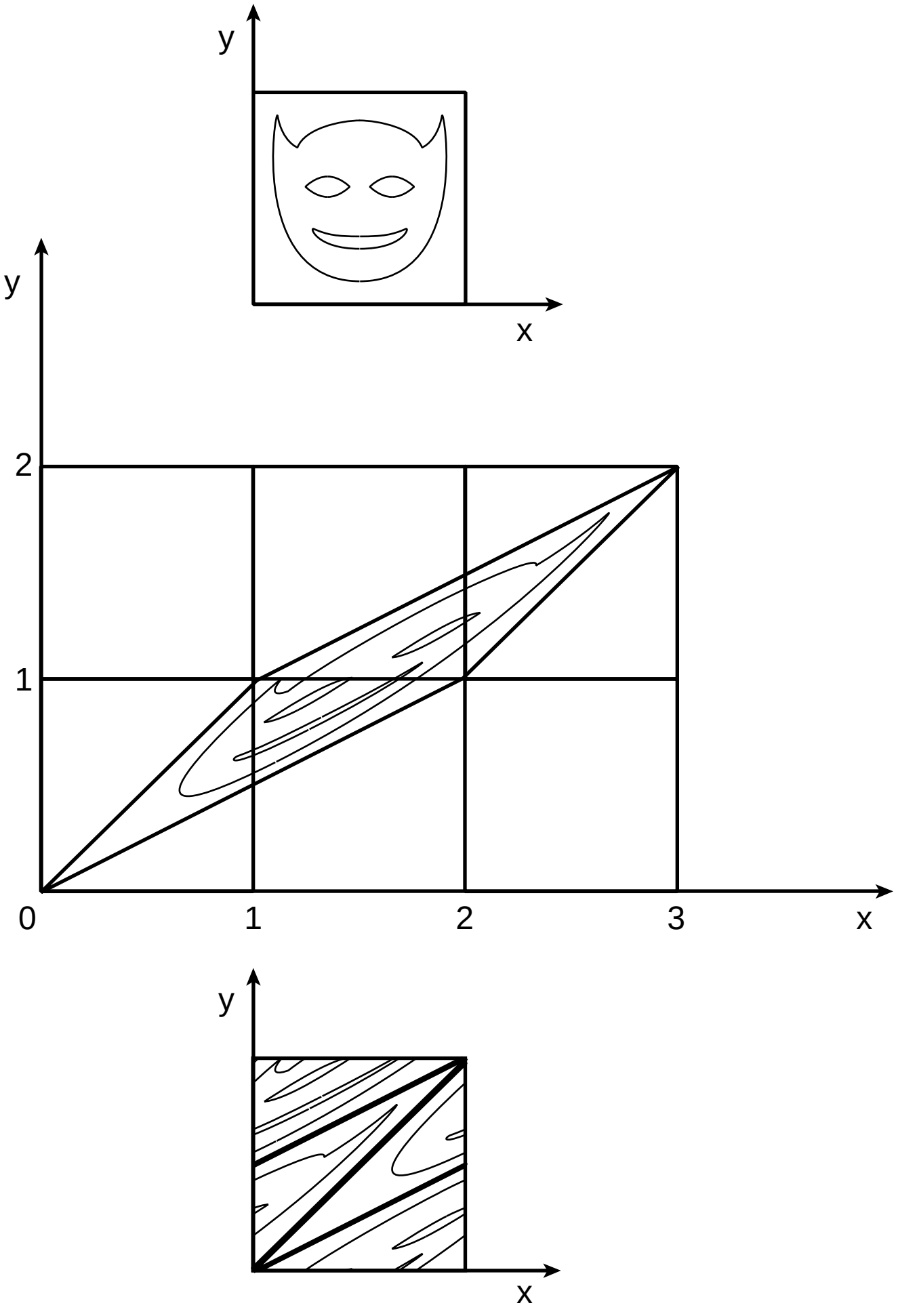
y
x
y
2
1
0
1
2
3
x
y
x

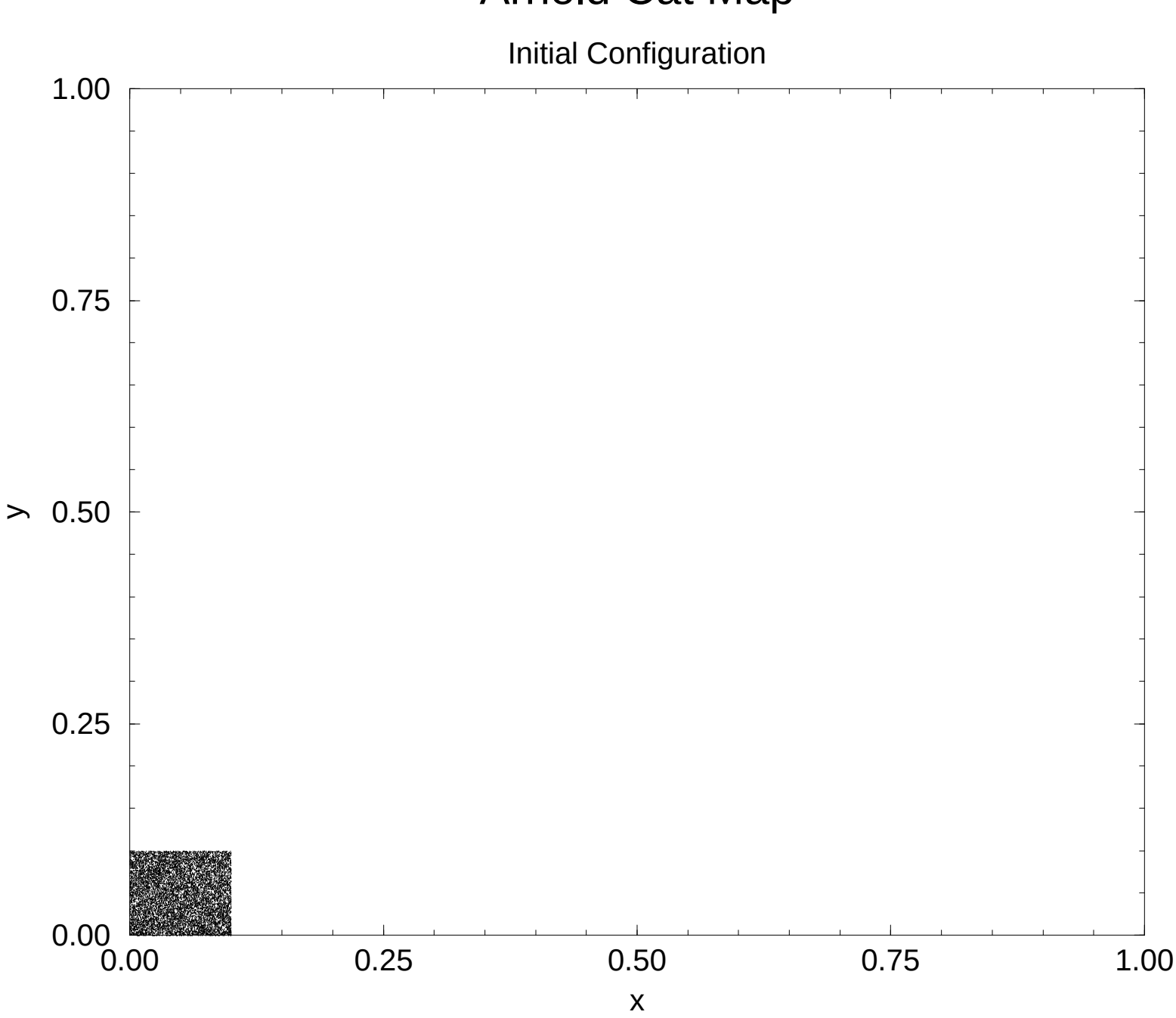
Arnold Cat Map
Initial Configuration
1.00
0.75
0.50
0.25
0.00
y
0.00
0.25
0.50
0.75
1.00
x

Arnold Cat Map

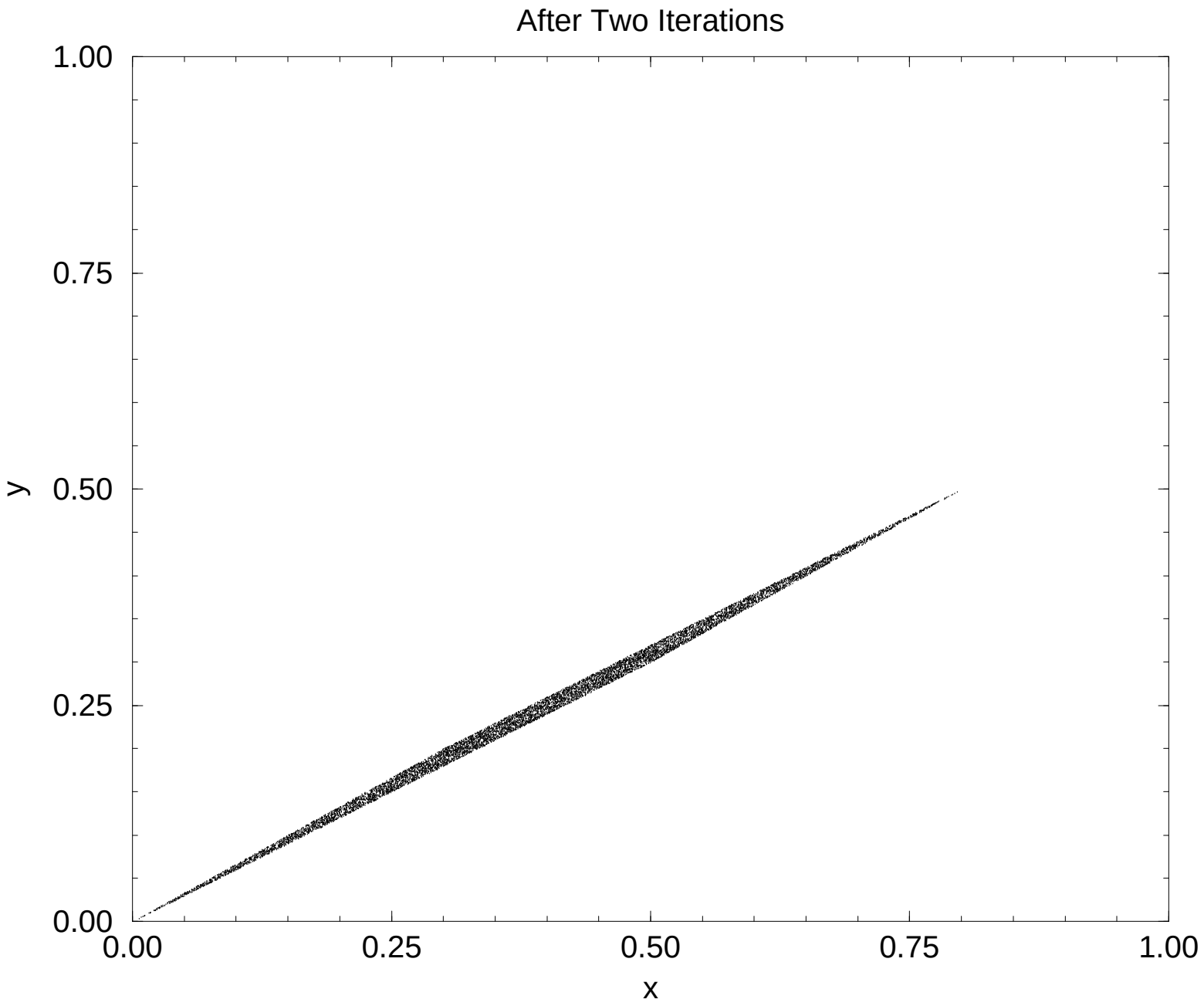

Arnold Cat Map

After Three Iterations

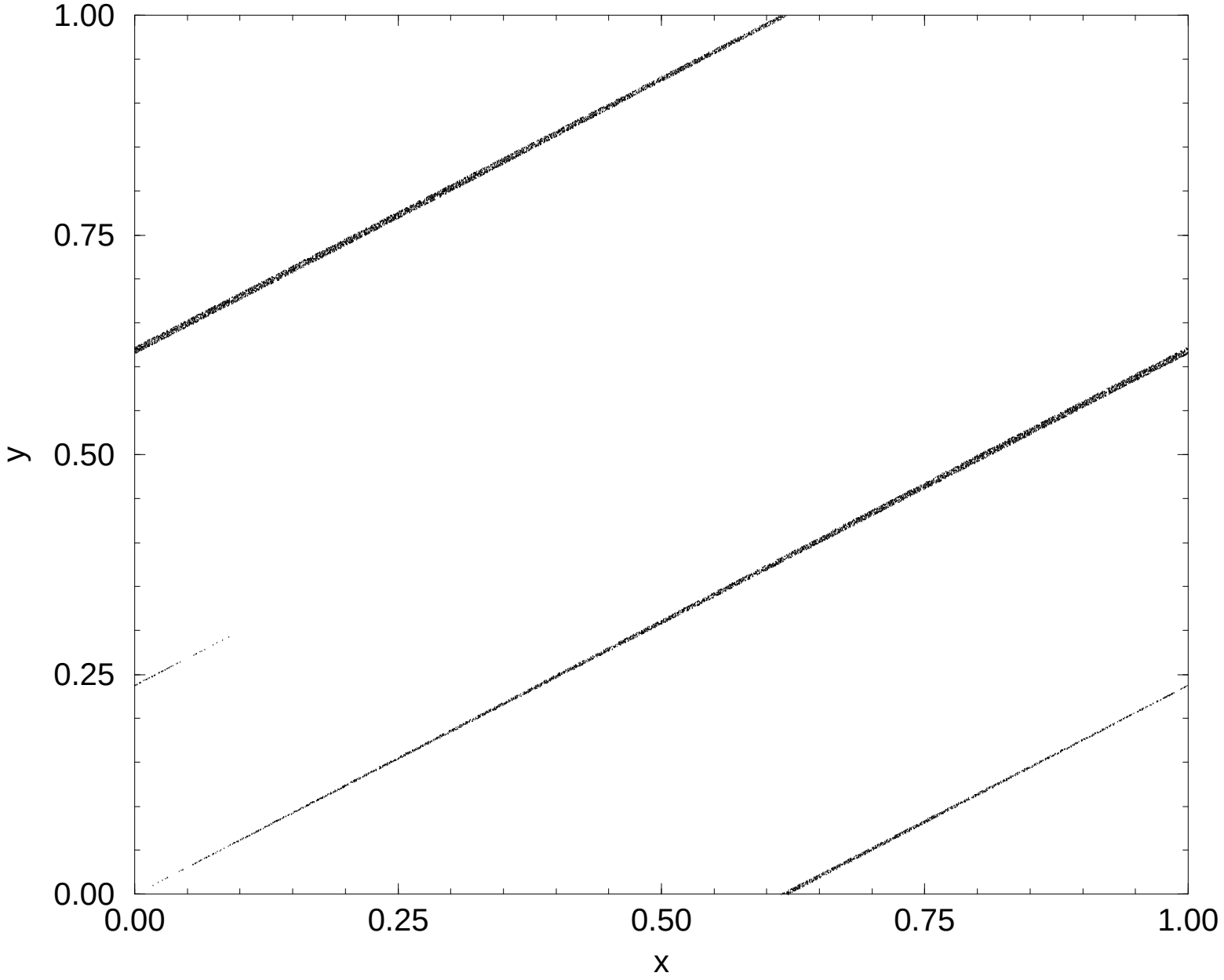

Arnold Cat Map

After Ten Iterations

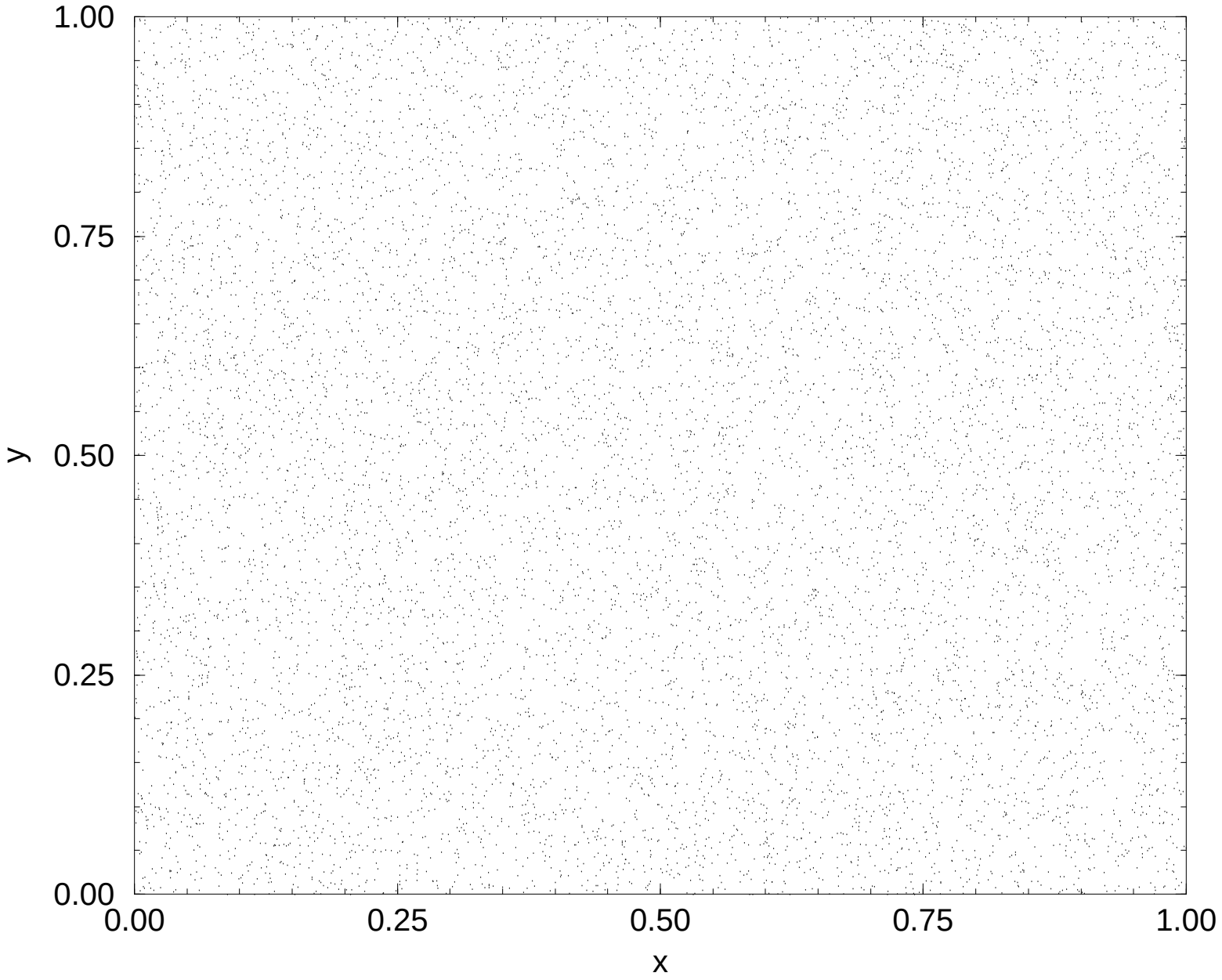

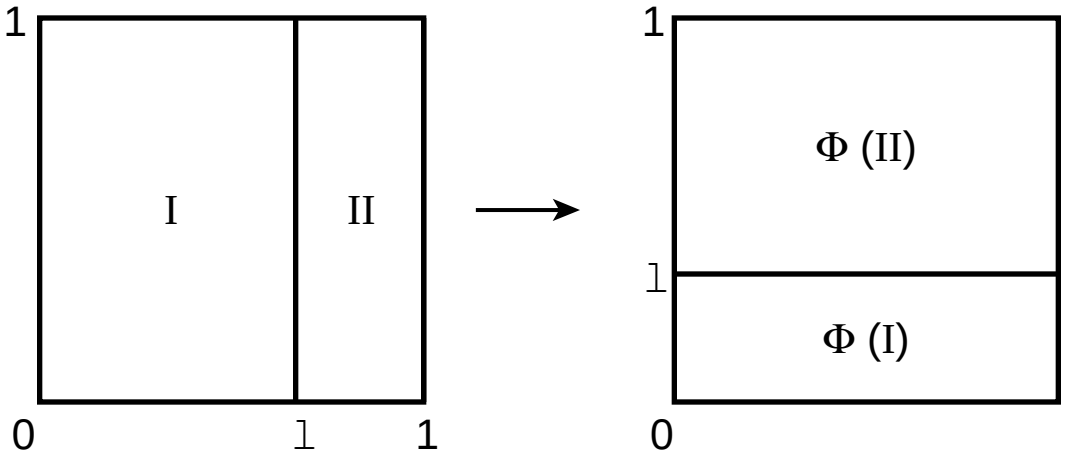
1
I
II
0
1
1
Φ (II)
1
Φ (I)
0

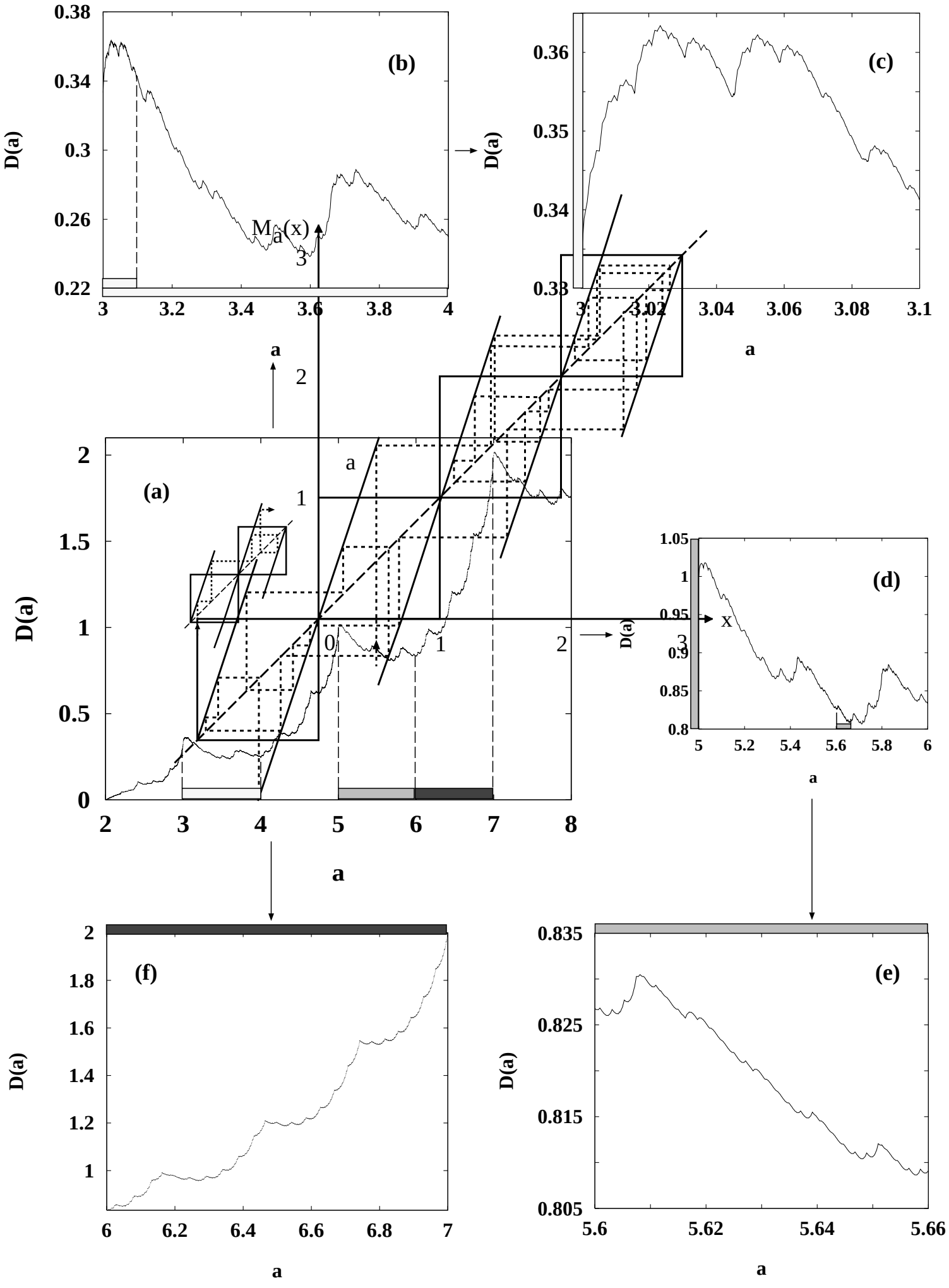
(a)
(b)
(c)
(d)
(e)
(f)
D(a)
a
x
$M_a(x)$
0
1
2
3

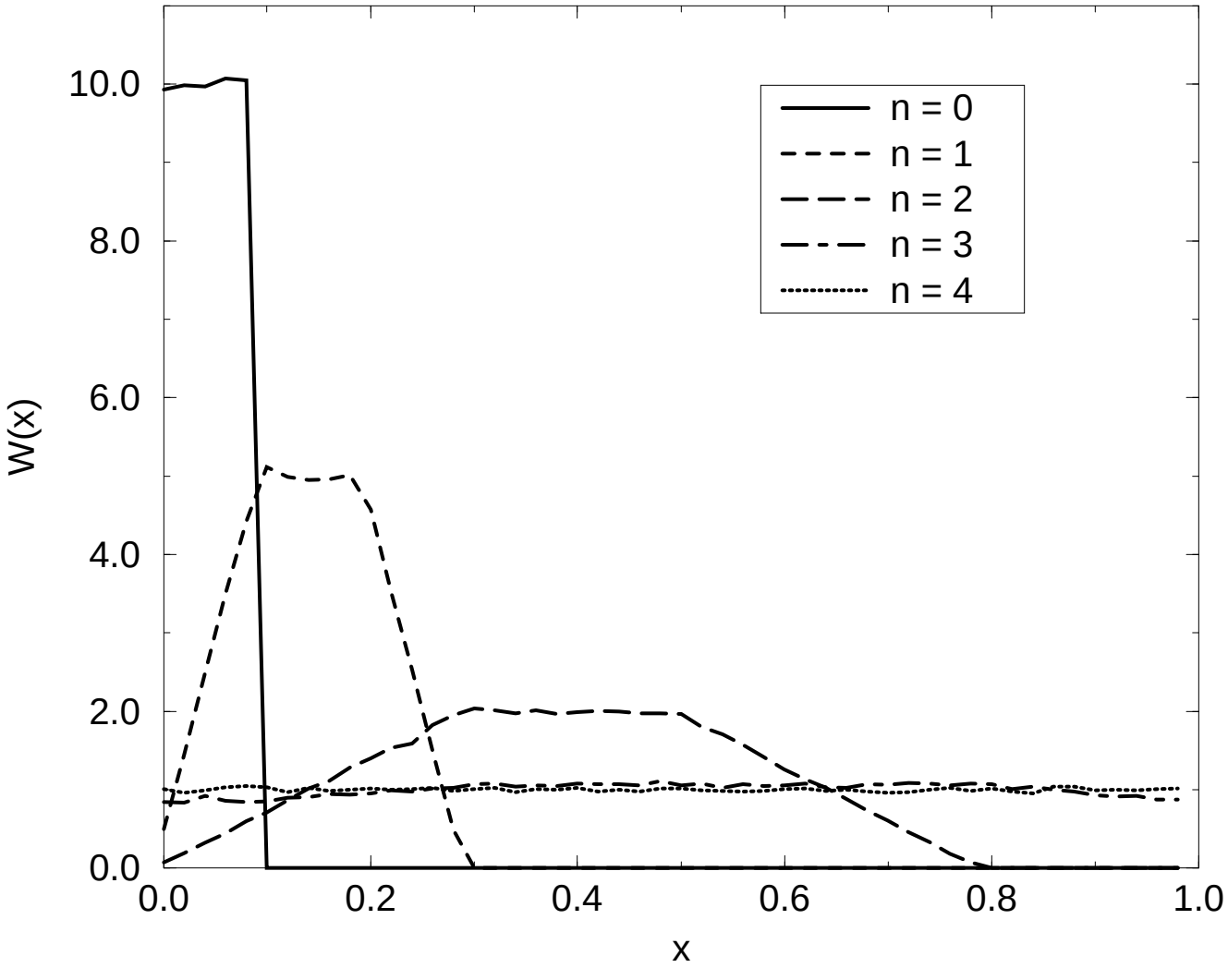
10.0
8.0
6.0
4.0
2.0
0.0
W(x)
0.0
0.2
0.4
0.6
0.8
1.0
x
n = 0
n = 1
n = 2
n = 3
n = 4

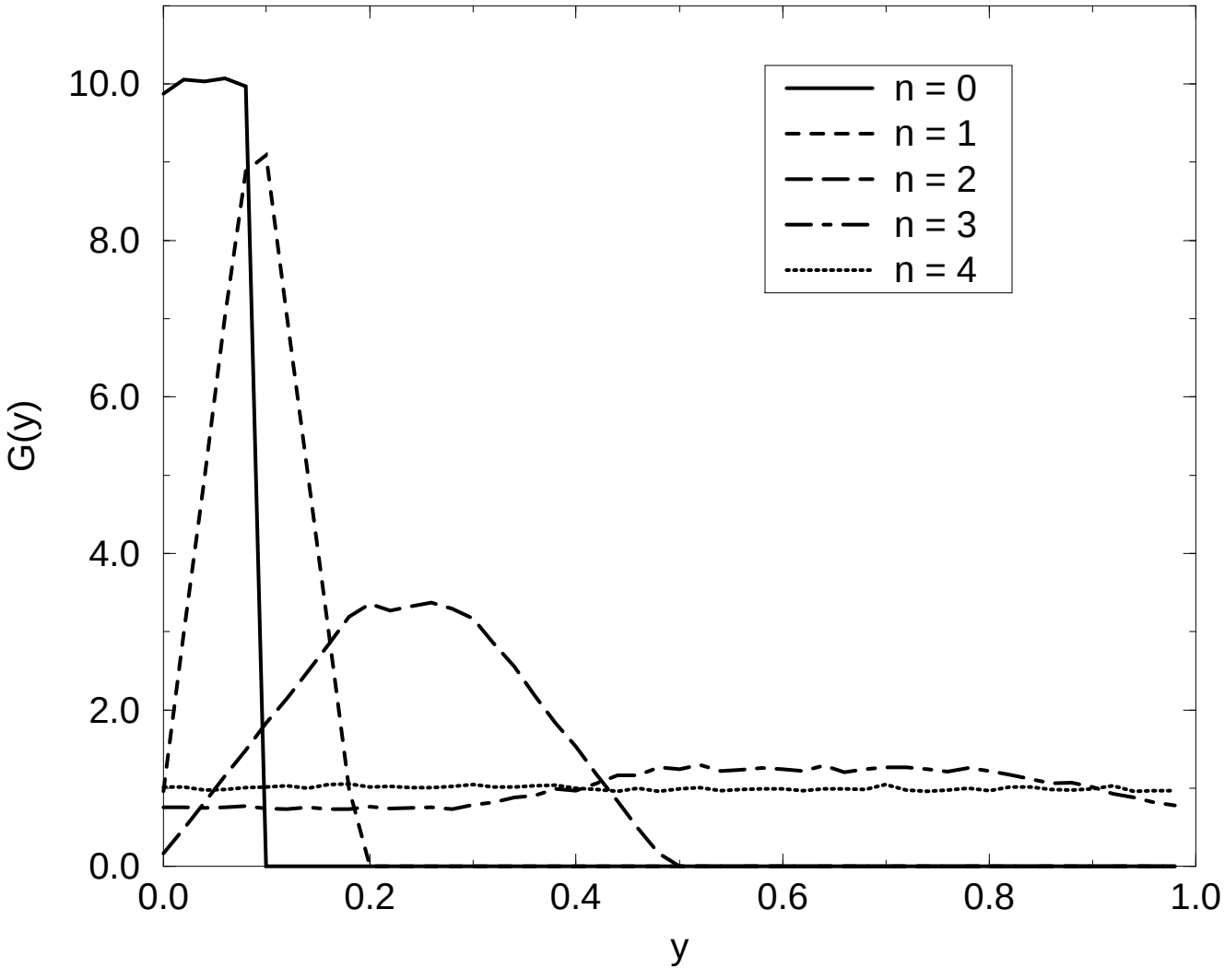
10.0
8.0
6.0
4.0
2.0
0.0
G(y)
0.0
0.2
0.4
0.6
0.8
1.0
y
n = 0
n = 1
n = 2
n = 3
n = 4

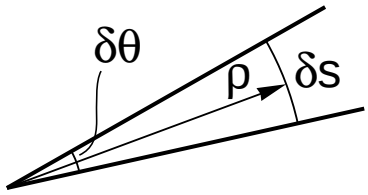
δθ
ρ
δs

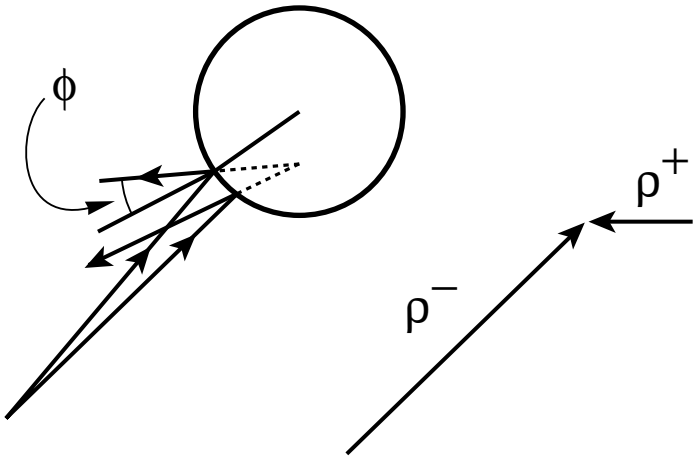
ϕ
ρ+
ρ−